UNIVERSIDAD DE CHILE

FACULTAD DE CIENCIAS FÍSICAS Y MATEMÁTICAS

DEPARTAMENTO DE INGENIERÍA CIVIL

ANÁLISIS DE SENSIBILIDAD DE PARÁMETROS DEL MODELO VIC A TRAVÉS DEL GRADIENTE HIDROCLIMÁTICO DE CHILE

TESIS PARA OPTAR AL GRADO DE MAGÍSTER EN CIENCIAS DE LA INGENIERÍA, MENCIÓN RECURSOS Y MEDIO AMBIENTE HÍDRICO

MEMORIA PARA OPTAR AL TÍTULO DE INGENIERO CIVIL

ULISES MATÍAS SEPÚLVEDA JILBERTO

PROFESOR GUÍA:

PABLO MENDOZA ZÚÑIGA

MIEMBROS DE LA COMISIÓN:

XIMENA VARGAS MESA

MIGUEL LAGOS ZÚÑIGA

SANTIAGO DE CHILE

2021

RESUMEN DE LA TESIS PARA OPTAR AL TÍTULO DE: Ingeniero Civil y grado de Magíster en Ciencias de la Ingeniería, mención Recursos y Medio Ambiente Hídrico
POR: Ulises Matías Sepúlveda Jilberto
FECHA: Septiembre de 2021
PROFESOR GUÍA: Pablo Mendoza Zúñiga

ANÁLISIS DE SENSIBILIDAD DE PARÁMETROS DEL MODELO VIC A TRAVÉS DEL GRADIENTE HIDROCLIMÁTICO DE CHILE

A pesar de que el modelo de Capacidad de Infiltración Variable (VIC) se ha utilizado durante décadas en la comunidad hidrológica, todavía hay una serie de parámetros cuyas sensibilidades siguen siendo desconocidas. La comprensión de los factores que controlan la sensibilidad paramétrica en el espacio es fundamental dado el creciente interés por mejorar la calibración de modelos distribuidos a alta resolución espacial, obteniendo distribuciones de parámetros continuas y coherentes. En este trabajo de tesis, se investigan las sensibilidades proporcionadas por 43 parámetros de suelo, vegetación y nieve del modelo VIC, en celdas de 0,05° × 0,05° contenidas dentro de 101 cuencas con régimen cercano al natural en Chile continental, con un total de 5.574 celdas. Se implementa un enfoque híbrido de análisis de sensibilidad local-global, utilizando ocho métricas de evaluación para caracterizar las sensibilidades paramétricas: cuatro de ellas son formuladas a partir de series de tiempo de caudal; dos caracterizan los procesos de la nieve y dos se basan en procesos de evaporación. Además, se realiza un análisis de correlación entre las sensibilidades paramétricas obtenidas y atributos climáticos y fisiográficos de las celdas, con el objetivo de identificar los principales factores que controlan la influencia de parámetros en respuestas hidrológicas simuladas.

Los resultados confirman una sobreparametrización para los procesos analizados, con sólo 12 parámetros (28% del total) definidos como sensibles: los parámetros de suelo *INFILT*; *Ws*; *Ds*; *DsMAX*; *Expt2*; *Depth2* y *Depth3*; los parámetros de vegetación *LAI* y *Rmin*; y los parámetros de nieve *NEWALB*; *ALBAA* y *ALBTHA*. Los análisis de correlación muestran que las variables climáticas – en particular, la precipitación media anual y el índice de aridez –, son los principales factores que controlan la sensibilidad de los parámetros. Por ejemplo, los parámetros *DsMAX* y *Ws* son relevantes para la pendiente del segmento medio de la curva de duración de caudales en zonas con mayor precipitación ($r_s = 0{,}91$) y bajo índice de aridez ($r_s = -0{,}91$), mientras que el parámetro *Rmin* es sustancial en el balance hídrico general en áreas con altas precipitaciones ($r_s = 0{,}85$), amplia fracción de cobertura de suelo definida como bosque ($r_s = 0{,}81$) e índices de aridez bajos ($r_s = -0{,}79$). Además, los resultados destacan la influencia del índice de área foliar en los procesos hidrológicos simulados, independientemente de los tipos de clima dominantes, y la relevancia de los parámetros de nieve codificados. En base a los resultados de la correlación y la interpretación de los patrones de sensibilidad espacial, se entrega una orientación sobre los parámetros más relevantes para la calibración del modelo VIC de acuerdo con los procesos objetivo y el tipo de clima predominante. En general, los resultados presentados contribuyen a una mejor comprensión del comportamiento del modelo para dominios con diversas características físicas, a lo largo de un pronunciado gradiente hidroclimático que abarca desde sistemas hiperáridos a húmedos.

TABLA DE CONTENIDO

ÍNDICE DE TABLAS

ÍNDICE DE FIGURAS

I. INTRODUCCIÓN

Durante las últimas cuatro décadas, los Modelos Tierra-Superficie (*Land Surface Models*; LSM) y los modelos hidrológicos distribuidos han surgido como herramientas poderosas para caracterizar el ciclo del agua. La historia de los modelos hidrológicos se remonta a mediados del siglo XIX, comenzando con modelos empíricos para predecir caudales máximos instantáneos (Todini, 2007). Durante mucho tiempo, los modelos hidrológicos se desarrollaron sólo para la escala de cuenca, evolucionando desde una base empírica hacia una base más física (Beven, 1989). El mayor poder computacional, la mayor disponibilidad de datos y una creciente necesidad por representar la heterogeneidad espacial y las características físicas de las cuencas hidrográficas han impulsado el desarrollo de modelos hidrológicos espacialmente distribuidos y cada vez más complejos (Boyle et al., 2001; Liu and Gupta, 2007; Nijssen and Bastidas, 2005; Sorooshian and Chu, 2013). Los modelos distribuidos pueden incorporar parámetros que varían espacialmente, reflejando heterogeneidades en la cubierta vegetal y las características del suelo (Carpenter and Georgakakos, 2006), además de la variabilidad espacial de las forzantes meteorológicas. En el contexto de la modelación climática, los modelos LSM pueden ser acoplados a Modelos de Circulación General y Modelos Climáticos Regionales para simular los procesos biofísicos involucrados en la interacción tierra-atmósfera (Wood et al., 2011), mientras que los modelos hidrológicos se enfocan en simular el caudal, centrándose en procesos hidrológicos como, por ejemplo, los mecanismos de generación de escorrentía; sin embargo, esta distinción entre modelos LSM y modelos hidrológicos se ha vuelto difusa con el tiempo (Clark et al., 2015)

El progresivo aumento en la complejidad de modelos hidrológicos de base física ha ido acompañado de un aumento en el número de parámetros ajustables, aumentando los tiempos de calibración (van Griensven et al., 2006; Muleta and Nicklow, 2005). En la actualidad, algunos valores de parámetros en modelos LSM son asignados mediante tablas de consulta para distintos tipos de suelo y vegetación. Sin embargo, estudios previos han demostrado que este procedimiento es demasiado simplista y puede generar una incertidumbre considerable (Hou et al., 2012; Rosero et al., 2010).

Con el fin de disminuir el costo computacional, el modelador generalmente elige un sub-set de parámetros "sensibles" para ser calibrados en base al juicio experto o a las recomendaciones de los desarrolladores del modelo (Rosero et al., 2009; Wang et al., 2018; Zhang et al., 2015). Sin embargo, la sensibilidad paramétrica de un modelo, así como el ranking de parámetros más importantes, pueden variar de una cuenca a otra dependiendo de características climáticas y fisiográficas. Por lo tanto, el análisis de sensibilidad es un requisito previo para mejorar la efectividad de la calibración del modelo hidrológico.

El análisis de sensibilidad se ha convertido en una herramienta útil para explorar espacios de parámetros de alta dimensión, evaluar la identificabilidad de parámetros, comprender las fuentes de incertidumbre y comprender la variabilidad de respuestas modeladas ante cambios en factores o parámetros. En este contexto, esta herramienta se usa comúnmente para determinar qué parámetros tienen un impacto sustancial en la respuesta del modelo y deberían ser el foco de los esfuerzos de calibración y, de manera paralela, qué parámetros tienen un leve impacto y cuyos valores, por lo tanto, podrían mantenerse constantes. Estudios de análisis de sensibilidad han incluido modelos hidrológicos como: *Biosphere-Atmosphere Transfer Scheme*, BATS (Bastidas et al., 1999); TOPKAPI (Foglia et al., 2009); *Precipitation Runoff Modeling System*, PRMS (Mendoza et al., 2015), Noah LSM (Bastidas et al., 2006; Rosero et al., 2010); Noah-MP (Cuntz

et al., 2016; Mendoza et al., 2015b), *Simple Biosphere Model*, SiB3 (Prihodko et al., 2008; Rosolem et al., 2012); *Modélisation Environmentale Communautaire - Surface and Hydrology*, MESH (Razavi and Gupta, 2016), *Community Land Model*, CLM (Göhler et al., 2013; Massoud et al., 2019) y, en particular, el modelo *Variable Infiltration Capacity*, VIC (por ejemplo, Demaria et al., 2007; Melsen et al., 2016), que es una de las plataformas de modelación más populares en la comunidad hidrológica (Addor and Melsen, 2019).

El modelo VIC se ha utilizado para innumerables aplicaciones en todo el mundo, incluido el modelamiento del manto nival (Andreadis et al., 2009; Chen et al., 2014), pronóstico de caudales (DeChant & Moradkhani, 2014; Wood et al., 2005), estudios de balance hídrico (DGA, 2017; Mizukami et al., 2016; Vásquez et al., 2021), caracterización de eventos extremos (Melsen et al., 2019); y evaluaciones de impacto del cambio climático (Chegwidden et al., 2019; Vano and Lettenmaier, 2014). En general, VIC incorpora más de 40 parámetros, algunos con sentido físico y otros 'libres' o ajustables. En algunos casos, los parámetros con importancia física se pueden ajustar de forma interactiva durante la calibración. Algunos parámetros pueden tener menos influencia en la salida del modelo, por lo que sus valores podrían fijarse de antemano, mientras que otros podrían generar mayores impactos. A medida que sigue existiendo interés en la comunidad por utilizar el modelo VIC y se siguen publicando actualizaciones (Hamman et al., 2018), la comprensión de su sensibilidad paramétrica cobra mayor importancia.

Desde su generalización como modelo de suelo de tres capas (VIC-3L; Liang et al., 1996), la sensibilidad del modelo a los parámetros del suelo ha sido analizada por varios autores. Por ejemplo, Liang & Guo (2003) evaluaron la sensibilidad de cinco parámetros en tres ubicaciones experimentales en flujos medios anuales como la escorrentía,, evapotranspiración (ET), la humedad del suelo y el flujo del calor sensible. Sus resultados indican que la sensibilidad de los parámetros varía con el clima, las propiedades del suelo y de la vegetación. Demaria et al. (2007) examinaron la sensibilidad de la respuesta en la escorrentía para cinco métricas de evaluación calculadas en cuatro cuencas con condiciones hidroclimáticas diferentes, logrando caracterizar la sensibilidad de los caudales simulados a los parámetros que controlan la generación de escorrentía superficial y subsuperficial. La sensibilidad a los cambios de uso de la tierra y los parámetros de vegetación asociados a las diferentes clases de vegetación (es decir, el índice de área foliar y el albedo) también se han explorado y expresado para los diferentes componentes de los balances hídricos y energéticos del modelo VIC (Bennett et al., 2018; Chawla and Mujumdar, 2015; VanShaar et al., 2002).

Estudios posteriores que han abordado la calibración del modelo VIC para simular respuestas a escala de cuenca han revisitado la sensibilidad paramétrica del modelo. Mendoza et al. (2015b) aplicaron el método de evaluación distribuida del análisis de sensibilidad local (DELSA por sus siglas en inglés; Rakovec et al., 2014) para encontrar los parámetros que proporcionan las mayores sensibilidades para la simulación de caudales altos en tres subcuencas de cabecera pertenecientes a la gran cuenca del río Colorado, encontrando que 9 parámetros entregaban las mayores sensibilidades, de un total de 34. Melsen et al. (2016) también utilizaron el método DELSA para encontrar parámetros influyentes en tres cuencas de Suiza, identificando cuatro de un total de 28 para tres métricas de calibración. Gou et al. (2020) caracterizaron la sensibilidad de 13 parámetros de suelo en 14 cuencas hidrográficas en China, encontrando que tres de ellos dominaron la respuesta en la escorrentía. Lilhare et al. (2020) aplicaron el método del análisis de variograma de superficies de respuesta (VARS; Razavi & Gupta, 2016) para examinar la sensibilidad a tres métricas de evaluación enfocadas en caudal en 10 cuencas de Canadá, hallando tres parámetros

sensibles de un total de 10. Finalmente, Yeste et al. (2020) cuantificaron las sensibilidades de cinco parámetros de suelo en los componentes del balance hídrico, concluyendo que dos parámetros controlan las respuestas.

Por otro lado, la escala a la que se lleva a cabo el análisis de sensibilidad suele depender del objetivo de la aplicación y de la escala de los datos de calibración. Dada la creciente disponibilidad de productos observacionales espacialmente distribuidos – y en particular de escorrentía (e.g., Do et al., 2018), algunos estudios han calibrado parámetros en cada celda de la cuadrícula para aumentar la densidad de calibración. Por ejemplo, Oubeidillah et al. (2014) recopilaron y organizaron datos clave para la simulación hidrológica, incluyendo forzantes meteorológicas, suelo, vegetación y elevación en cuadriculas refinadas de 1/24° (~4 km) para realizar una calibración espacialmente consistente del modelo VIC en Estados Unidos. Troy et al. (2008) investigaron los efectos de calibrar en celdas de 1°, 1/2°,1/4° y 1/8° sobre la transferencia del conjunto de parámetros a otras resoluciones espaciales. Yang et al. (2019) calibraron tres parámetros del modelo VIC en celdas de 1/8°, y evaluaron el modelo con una resolución ligeramente mayor que 1/16°.

En este trabajo de tesis, se caracteriza la sensibilidad paramétrica del modelo VIC a la escala de celda, utilizando distintas métricas y un conjunto de parámetros estándar y codificados (i.e., considerados constantes por los desarrolladores). Específicamente, se abordan las siguientes preguntas:

1. ¿Cuántos y qué parámetros del modelo VIC son redundantes?

2. ¿Qué factores climáticos y fisiográficos determinan la magnitud de la sensibilidad paramétrica con respecto a procesos hidrológicos específicos?

Objetivos generales

El objetivo general es aplicar el método DELSA (Rakovec et al., 2014) para caracterizar la sensibilidad paramétrica del modelo VIC a través del gradiente hidroclimático de Chile, utilizando diversas métricas de evaluación enfocadas en diferentes procesos hidrológicos.

Objetivos específicos

- Determinar cómo la sensibilidad paramétrica se relaciona con distintos procesos hidrológicos (caracterizados con diferentes métricas).
- Determinar si se justifica una complejidad moderada del modelo VIC (o se demuestra que es excesiva).
- Generar una guía de parámetros relevantes en función de las métricas evaluadas y las características hidroclimáticas dominantes.

Estructura del documento

Este documento está organizado de la siguiente forma: En el capítulo II se presenta el borrador del artículo para publicación y en el capítulo III se exponen las conclusiones del trabajo de tesis.

II. ARTÍCULO PARA PUBLICACIÓN

A continuación, se presenta el artículo titulado: "*Revisiting parameter sensitivities in the Variable Infiltration Capacity model*":

Revisiting parameter sensitivities in the Variable Infiltration Capacity model

Ulises M. Sepúlveda[1] and Pablo A. Mendoza[1,2]

1. Department of Civil Engineering, Universidad de Chile, Santiago, Chile
2. Advanced Mining Technology Center (AMTC), Universidad de Chile, Santiago, Chile

Corresponding author: Ulises M. Sepúlveda (ulises.sepulveda@ug.uchile.cl)

Keywords: parameter sensitivity, sensitivity analysis, DELSA, VIC model, hydrological processes

Key points:

- We conduct sensitivity analysis on 43 parameters of the Variable Infiltration Capacity model on a grid-by-grid basis.
- Process-based sensitivities reveal differences among parameters, and discrepancies in spatial sensitivity patterns.
- We provide guidance on relevant parameters depending on the target processes and climate types.

Abstract

Despite the Variable Infiltration Capacity (VIC) model has been used for decades in the hydrology community, there is still several parameters whose sensitivities remain unknown. Understanding the factors that control parameter sensitivities in space is critical given the increasing interest to improve calibration density with spatially coherent parameter fields. In this study, we investigate the sensitivities provided by 43 soil, vegetation and snow parameters, in the VIC model, at every 0.05 ° × 0.05 ° grid cell contained within 101 catchments across continental Chile, with a total of 5,574 grid cells. We implement a hybrid local-global sensitivity analysis approach, using eight evaluation metrics to characterize sensitivities, with four of them formulated from runoff time series; two characterizing snow processes, and the remaining two based on evaporation processes. Our results confirm an over-parameterization for the processes analyzed here, with only 12 parameters (i.e., 28%) defined as sensitive (i.e., *INFILT*; *Ws*; *Ds*; *DsMAX*; *Expt2*; *Depth2*; *Depth3*; *LAI*; *Rmin*; *NEWALB*; *ALBAA* and *ALBTHA*). Correlation analyses show that climate variables – in particular, mean annual precipitation and aridity index – are the main controls on parameter sensitivities. Additionally, our results highlight the influence of the leaf area index on simulated hydrologic processes – regardless on the dominant climate types – and the relevance of hard-coded

snow parameters. Based on correlation results and the interpretation of spatial sensitivity patterns, we provide guidance on the most relevant parameters for model calibration according to the target processes and the prevailing climate type. Overall, the results presented here contribute to improved understanding of model behavior across watersheds with diverse physical characteristics that encompass a wide hydroclimatic gradient from hyper-arid to humid systems.

1 Introduction

Over the past four decades, the increasing demand for more realistic spatial representations of water storages and fluxes across large domains has motivated the development of more complex physics-based models (e.g., Clark et al., 2015; Lawrence et al., 2019; Niu et al., 2011). The progress in this field has been partly facilitated by new observational datasets (e.g., Berg et al., 2018; McCabe et al., 2017) and advances in computing (see discussion on tradeoffs in Clark et al., 2017), enabling hydrological characterizations at the national (e.g., Tian et al., 2017; Zink et al., 2017), continental (e.g., Abbaspour et al., 2015; Xia et al., 2012) and global (e.g., Arheimer et al., 2020; Schmied et al., 2014) scales.

Large domain applications require the specification of parameter values to reflect spatial heterogeneities in landscape properties. Because increasing model complexity is often associated with a larger number (>30) of parameters, many models rely on lookup tables to assign soil thermal and hydraulic parameters, and vegetation optical and physiological parameters to each modeling unit (e.g., Mitchell et al., 2004; Yang et al., 2011). However, parameter uncertainties may be considerable (Hou et al., 2012; Rosero et al., 2010), and such problem is exacerbated by the existence of parameters that, despite being "adjustable" (e.g., runoff generation parameters), remain fixed and hard-coded (e.g., Cuntz et al., 2016; Mendoza et al., 2015a).

To address overparameterization problems that are typical in environmental models, sensitivity analysis has become a key tool that provides information on which parameter values are the most influential for the dynamics of specific model responses (Razavi and Gupta, 2015). The outcomes of sensitivity analysis not only help to improve understanding on model functioning, but also to inform decisions regarding parameter estimation problems. The literature provides many examples of sensitivity analysis studies with process-based hydrological models, including the Biosphere-Atmosphere Transfer Scheme, BATS (Bastidas et al., 1999); TOPKAPI (Foglia et al., 2009); PRMS (Mendoza et al., 2015b), the Noah land surface model (Bastidas et al., 2006; Rosero et al., 2010); Noah-MP (Cuntz et al., 2016; Mendoza et al., 2015a), the Simple Biosphere model, SiB3 (Prihodko et al., 2008; Rosolem et al., 2012); the MESH modeling system (Razavi and Gupta, 2016), the Community Land Model, CML (Göhler et al., 2013; Massoud et al., 2019) and the Variable Infiltration Capacity (VIC) model (e.g., Demaria et al., 2007; Melsen et al., 2016), which is one of most popular modeling platforms in the hydrology community (Addor and Melsen, 2019).

The VIC model (Hamman et al., 2018; Liang et al., 1994) has been used for myriad applications all over the world, including snow modeling (Andreadis et al., 2009; Chen et al., 2014), streamflow forecasting (DeChant & Moradkhani, 2014; Wood et al., 2005), water balance studies (Mizukami et al., 2016; Vásquez et al., 2021), extreme event characterization (Melsen et al., 2019); land use change impacts (Chawla and Mujumdar, 2015) and climate change impact assessments (e.g., Chegwidden et al., 2019; Vano and Lettenmaier, 2014). Despite the large number of parameters contained in VIC – either 'free' (e.g., the infiltration shape parameter '*INFILT*', the exponent in baseflow curve) or 'observable' (e.g., leaf area index) –, many studies have relied on the calibration

of two or three soil-related parameters (Chawla and Mujumdar, 2015; Huang and Liang, 2006). Conversely, other authors have advocated for characterizing parameter sensitivities using different approaches, sensitivity metrics, and including different parameters. For example, Liang & Guo (2003) assessed the sensitivity of annual runoff, annual evapotranspiration (ET), annual mean soil moisture, and annual mean sensible heat flux to variations in five soil and vegetation parameters at three experimental locations (i.e., point scale), finding that sensitivities varied with climatic and physiographic site characteristics. Demaria et al. (2007) examined sensitivities in simulated catchment-scale runoff responses using lumped VIC configurations, a Monte Carlo method, and five objective functions computed for four basins with varying hydroclimates. They concluded that (i) three (out of ten) soil parameters dominated the simulated runoff response; (ii) the *INFILT* parameter and the drainage parameter ($Expt_i$) depended strongly on local hydroclimatology, and (iii) that the baseflow model formulation is overparameterized.

Subsequent studies aiming at calibrating the VIC model to simulate observed catchment-scale responses have revisited its parametric sensitivity. Mendoza et al. (2015b) applied the distributed evaluation of local sensitivity analysis method (DELSA, Rakovec et al., 2014) to find the parameters that provided the largest sensitivities in root mean squared errors (RMSE) between simulated and observed streamflow; they showed that 9 (out of 34) parameters provided the largest sensitivities in three subcatchments from the Upper Colorado River basin. Melsen et al. (2016) also used the DELSA method to find influential parameters in three catchments located in Switzerland, identifying four (out of 28) very sensitive parameters for three calibration metrics. Wi et al. (2017) applied the method of Morris (1991) to quantify parameter sensitivities on the Nash-Sutcliffe efficiency (NSE; Nash and Sutcliffe, 1970) with daily flows, finding 6 soil parameters and two temperature threshold parameters as the most influential (out of 15). Gou et al. (2020) characterized the sensitivities provided by 13 soil parameters across 14 catchments in China, finding that *INFILT*, *Depth1* and *Depth2* dominated streamflow responses. Lilhare et al. (2020) applied the Variariogram Analysis of Response Surfaces (VARS) method (Razavi and Gupta, 2016) to examine the sensitivities of three streamflow performance metrics to variations in six soil parameters across 10 catchments in Canada, finding that *INFILT* and *Depth2* parameters dominated streamflow responses. Finally, Yeste et al. (2020) quantified relative sensitivities provided by five soil parameters to water balance components across 31 basins in the Iberian Peninsula, concluding that *INFILT* and *Depth2* control runoff components and evapotranspiration (ET).

Table 1 summarizes the main characteristics of parameter sensitivity studies with VIC. One can note that most of them focused on streamflow responses, attributing the largest sensitivities to a few soil parameters (Demaria et al., 2007; Gou et al., 2020; Lilhare et al., 2020). Only two studies – also characterizing streamflow responses – have included a large number of soil, vegetation and snow related parameters (Melsen et al., 2016; Mendoza et al., 2015b). Interestingly, only one study (Chaney et al., 2015) aimed to characterize sensitivities across 1° resolution grid cells, quantifying the effects of 9 parameters on annual flow biases, runoff seasonality and daily flow extremes across the globe. Sensitivity analyses at such scale and lower resolutions is particularly relevant for the hydrology community, considering recent developments in global, gridded runoff datasets (e.g., Do et al., 2018; Ghiggi et al., 2019) and the increasing interest to improve the calibration density in distributed hydrology and land surface models (Yang et al., 2019).

In this paper, we quantify VIC parameter sensitivities across 5,574 grid cells (0.05°×0.05°) covering 101 catchments located in continental Chile, including a suite of 43 standard and hard-

coded parameters, and a set of metrics that span different runoff, ET and snow processes. With this, we seek to answer the following research questions:

1. Are there other vegetation and snow parameters, either standard or hard-coded, affecting simulated runoff responses in VIC?
2. What are the effects of standard and hard-coded parameters on other simulated processes?
3. How do parameter sensitivities relate with local climatic and physiographic characteristics?

Table 1. Summary of sensitivity analysis studies conducted with VIC, that incorporate at least five parameters[a].

Study	Region	Number of sites or catchments	Target variables or metrics	Number of parameters included in SA	Methods	Most sensitive parameters
Liang & Guo (2003)	Red-Arkansas River basin, USA	3 sites	Annual runoff, annual ET, annual mean soil moisture, and annual mean sensible heat flux	5 pre-defined parameters	Fractional Factorial Analysis (FFA)	Varied with site characteristics
Demaria et al. (2007)	South-East of the United States	4 catchments	Five metrics (including RMSE, bias and correlation) formulated with daily streamflow and daily baseflow	10 soil parameters	Regional Sensitivity Analysis	INFILT, $Expt_i$ and Depth2
Chaney et al. (2015)	Global	1° resolution grid cells over the globe excluding Greenland and Antarctica (15,836 grid cells in total).	Annual flow biases, runoff seasonality and daily flow percentiles.	8 soil and one vegetation parameter	Distance between a priori CDF and behavioral parameter CDF	INFILT, DsMAX, $Expt_i$, and Rmin for annual biases; INFILT and DsMAX when adding the monthly constraint; INFILT, DsMAX, $Expt_i$, and Rmin dominate daily flow extremes.
Mendoza et al. (2015b)	Colorado Headwaters Region, USA	3 headwater basins	RMSE(Q) with Q at daily time steps	34 soil, vegetation and snow parameters	DELSA	INFILT, Ds, DsMAX, Ws, Depth2, Depth3, NEWALB, ALBAA, ALBTHA
Melsen et al. (2016)	Thur basin, Switzerland	3 catchments	NSE(Q), KGE(Q) and KGE(log(Q)) with Q at daily and hourly time steps	28 soil, vegetation and snow parameters	DELSA	INFILT, Ds, Expt2, DsMAX
Wi et al. (2017)[b]	American River basin, USA	1 catchment (North Fork sub-basin)	NSE(Q) with Q at daily time steps	15 soil, snow and routing parameters	Morris	INFILT, Ds, DsMAX, Ws, Depth 1, Depth2, Depth3, snow Tmax & Tmin
Gou et al. (2020)	10 major river basins in China	14 catchments	NSE(Q) with Q at monthly time steps	13 soil parameters	Three qualitative (SOT, MARS, DT) and one	INFILT, Depth1 and Depth2 are the overall most influential

Study	Region	Number of sites or catchments	Target variables or metrics	Number of parameters included in SA	Methods	Most sensitive parameters
					quantitative (Sobol') method	parameters on streamflow
Lilhare et al. (2020)	Lower Nelson River basin, Canada	10 sub-basins	NSE(Q), KGE(Q) and PBIAS(Q) with Q at daily time steps	6 soil parameters	VARS	INFILT and Depth2 arised as the most sensitive parameters. Relative importance depends on the catchment.
Yeste et al. (2020)	Duero River basin, Iberian Peninsula	31 headwater basins	Temporal averages of surface runoff, baseflow, total runoff, ET, and total soil moisture	5 soil parameters	SRC	Surface runoff, baseflow, total runoff, ET and SM1 are mainly sensitive to INFILT and Depth2. SM2 affected mostly by Depth2, and SM3 affected by Ds, DsMAX and Ws
This study	Continental Chile	5,574 grid cells (0.05°×0.05°)	8 metrics computed at daily time steps	43 soil, vegetation and snow parameters	DELSA	INFILT, Ds, DsMAX, Ws, Expt2, Depth2, Depth3, Rmin, LAI, NEWALB, ALBTHA, ALBAA

[a]The studies are listed in order of publication date. The present study has been added for completeness.
[b]We exclude two routing parameters that were found sensitive, but were not used in the other studies.
FFA: Factorial Fractional Analysis (Montgomery, 1991)
DELSA: Distributed Evaluation of Local Sensitivity Analysis (Rakovec et al., 2014).
DT: Delta test (Pi and Peterson, 1994).
SOT: Sum-Of-Trees model (Chipman et al., 2010).
MARS: Multivariate Adaptive Regression Splines (Friedman, 1991).
VARS: Variariogram Analysis of Response Surfaces (Razavi and Gupta, 2016).
SRC: Standardized Regression Coefficients (Saltelli et al., 2008)

2 Study domain and data

In this work, we select 101 catchments with near-natural hydrological regimes from the CAMELS-CL data set (Alvarez-Garreton et al., 2018). The selected basins span a total area of 139,350 km^2 – i.e., 19% of the territory of continental Chile –, and meet the following criteria: (i) a maximum threshold value of 5% for the relationship between the annual volume of water assigned as permanent consumptive rights and the average annual flow (Table 3 in Alvarez-Garreton et al., 2018), and (ii) absence of large reservoirs within each catchment. The location, hydroclimatic and land cover characteristics of the selected basins are shown in Figure 1, and catchment descriptors are listed in Table 2. These catchments cover a wide range of physiographic attributes, with drainage areas spanning 100-7,500 km^2, mean elevations ranging 119 - 4824 m above sea level, mean slopes varying from 52 to 306 m km^{-1}, and markedly different land cover types, ranging from completely covered by native forest or grassland to fully covered by impermeable land. Moreover, the selected basins represent the diversity in hydroclimatological conditions across the country. For example, the hydrology of catchment 2101001 (Rio Loa before Lequena dam, Figure 2a) is influenced by arid conditions between March and November, and Altiplanic winter events triggering runoff increases between December and March; towards the south, there is a transition

from arid to semi-arid conditions (see progression in Figure 2b-c), with precipitation events occurring mostly during winter, favoring the accumulation of snow in the headwaters of Andean catchments, and thus snowmelt-driven regimes. Catchments 7115001 (Palos River at junction with Colorado River; Figure 2d) and 8317001 (Biobio River at Rucalhue; Figure 2e) reflects the transition towards mixed regimes, with larger contributions of winter rainfall events to runoff. Finally, catchment 9129002 (Cautin River at Cajon; Figure 2f) has a rainfall-dominated hydrological regime.

Table 2. List of physiographic and hydroclimatic attributes used to characterize model grid cells.

Predictor	Class	Description	Data source
Elevation	Topographic	Mean elevation (m.a.s.l.)	DGA (2017)
Slope	Topographic	Mean topographic slope (°)	SRTM DEM
Precipitation	Climate	Mean annual precipitation (mm/yr)	CR2MET (Boisier et al., 2018) (https://www.cr2.cl/)
Temperature	Climate	Mean temperature (°C)	CR2MET (Boisier et al., 2018) (https://www.cr2.cl/)
Humidity	Climate	Mean relative humidity (-)	CR2MET (Boisier et al., 2018) (https://www.cr2.cl/)
Aridity	Climate	Aridity index (-), ratio of long-term potential evaporation to precipitation	-
Clay	Soil	Soil clay content (%) average over all layers	SoilGrids250m (Hengl et al., 2017) (https://soilgrids.org/)
Bare soil	Land cover	Fraction of bare soil	DGA (2017)
Forest	Land cover	Fraction of forest	DGA (2017)
Grasslands	Land cover	Fraction of grasslands	DGA (2017)
Shrub	Land cover	Fraction of shrub	DGA (2017)
Snow	Land cover	Fraction of snow cover	DGA (2017)

In this study, meteorological forcing data is obtained from various sources. Time series of daily precipitation and maximum, average, and minimum daily temperature are obtained from the CR2MET meteorological dataset, introduced in DGA (2017), which provides data for continental Chile at a horizontal resolution of 0.05°×0.05° (~5 km) for the period 1979-2016. The precipitation product builds upon a statistical post-processing technique that uses topographic descriptors and simulated meteorological variables from ERA-Interim (Dee et al., 2011) and ERA5 (Copernicus Climate Change Service, 2017) as predictors, and daily precipitation records as the predictand. A similar approach is used to generate time series of daily maximum and minimum temperatures, including additional predictors from MODIS land surface products. Daily precipitation and temperature variables are disaggregated into 3-hourly time steps using the sub-daily distribution provided by ERA-Interim. Finally, relative humidity and wind speed were obtained from a blend between ERA-Interim and ERA5, which was subsequently rescaled at the CR2MET horizontal grid through spatial interpolation. It is important to note that this product combination was created because ERA5 was not available during the entire study period (1985-2015) at the time of data acquisition (early 2018, where only 2010-2016 data was available). However, the updated reanalysis information, despite the short time coverage, was included due to various developmental improvements.

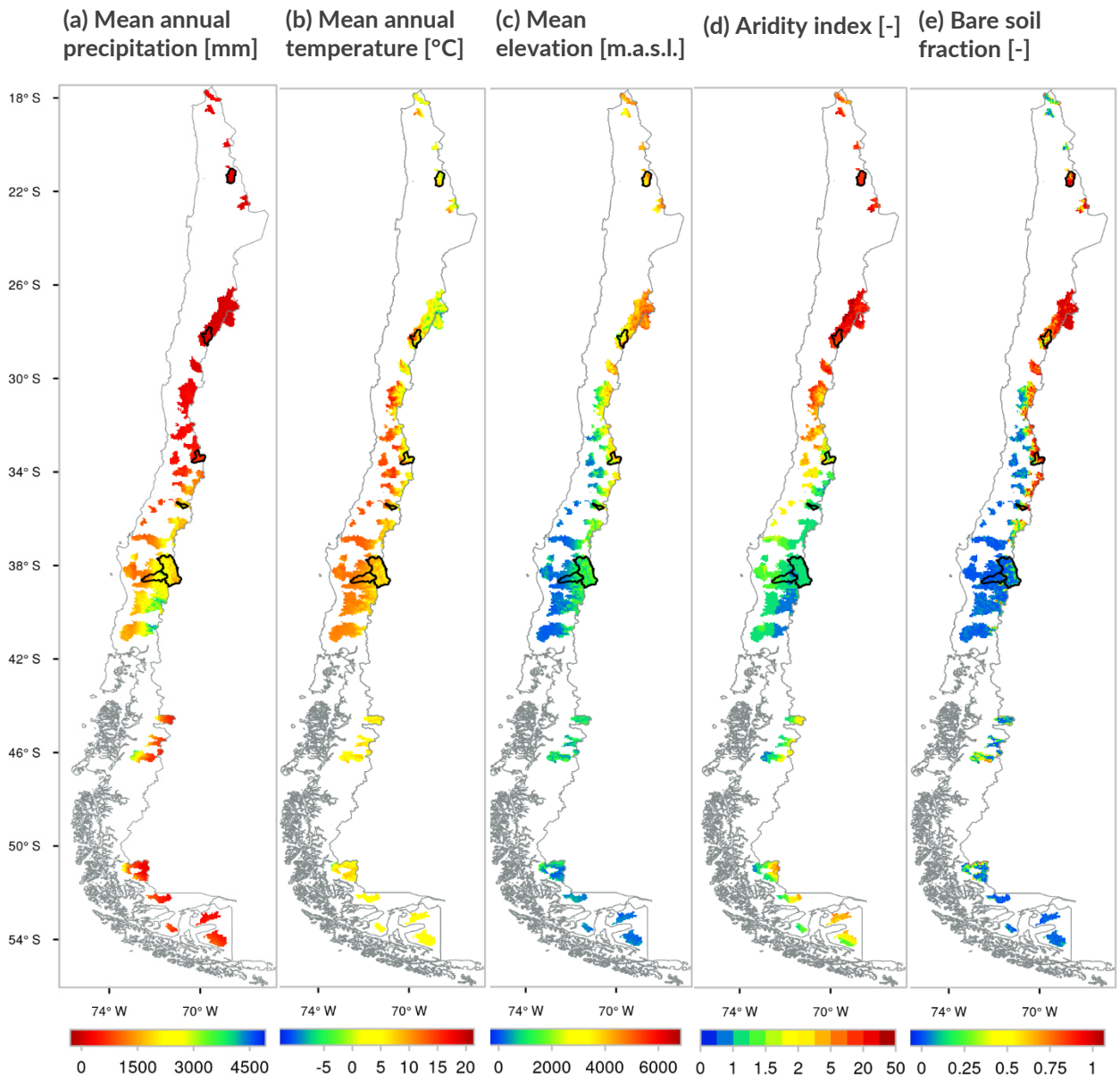

Figure 1. Spatial distribution of climatic and physiographic attributes across all grid cells: (a) mean annual precipitation (period 1979 – 2020), (b) mean annual temperature (period 1979 – 2020), (c) mean elevation, (d) aridity index and (e) bare soil fraction.

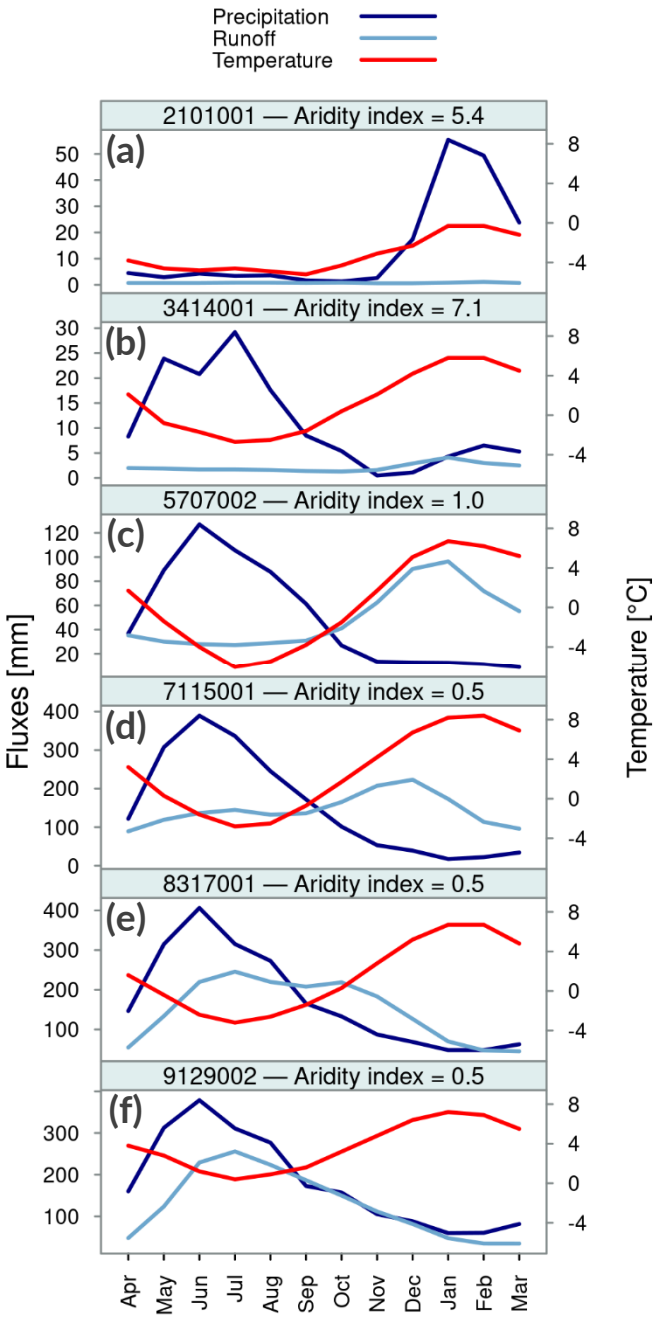

Figure 2. Seasonal cycles of catchment-averaged precipitation, runoff and temperature (period 1981 – 2018) for six basins representative of the hydroclimatic diversity within the study domain. From north to south: (a) Loa River upstream Lequena reservoir; (b) Pulido River at Vertedero; (c) Colorado River before junction with Maipo River; (d) Palos River at junction with Colorado River; (e) Biobío River at Rucalhue; (f) Cautin River at Cajon.

3 Methods

3.1 Hydrological model

The Variable Infiltration Capacity (Liang et al., 1994, 1996) model is a semi-distributed, physically-based hydrological model that simulates snow accumulation and melt, evapotranspiration (ET), canopy interception, surface runoff, baseflow, and other hydrological processes at daily or sub-daily time steps. In VIC, the domain of interest can be spatially discretized into grid cells. Sub-grid land-use type variability is accounted for by providing vegetation tiles and the fractional areas, for which water and energy balance equations are solved separately; then, model states and fluxes are spatially averaged to provide results at the pixel scale. In VIC, each grid cell can have up to three soil layers: the two top layers represent the interaction between moisture and vegetation, and the bottom soil layer is used to simulate baseflow processes. It should be noted that VIC does not incorporate an aquifer at the bottom of the soil column, nor lateral exchange of fluxes between grid cells. Finally, snowpack dynamics are simulated by a two-layer mass and energy balance model (Andreadis et al., 2009; Cherkauer et al., 2003), where the surface layer solves the energy exchange between the snowpack and the atmosphere, and the lower layer stores the excess snow mass from the upper surface layer.

3.2 Parameters considered for sensitivity analysis

We considered a suite of 43 parameters (Table 3) to incorporate

most of soil, vegetation, and snow processes simulated by VIC. It should be noted that three of the snow parameters are not exposed to model users (*NEWALB*, *ALBAA* and *ALBTHA*). For those parameters that show monthly variations, we examined sensitivities using regularization "superparameters" (Tonkin and Doherty, 2005), also called multipliers (Pokhrel and Gupta, 2010), which are uniformly applied over all monthly values. Hence, multipliers are used for the leaf area index (*LAI*); vegetation albedo (*ALB*); vegetation roughness length (*ROU*) and vegetation displacement (*DIS*).

Despite the aim to include the largest possible number of parameters, some of them were discarded for different reasons. For example, a few soil parameters (e.g., soil bubbling pressure) are not active unless the frozen soil algorithm is turned on. We also excluded the parameter trunk_ratio – i.e., the ratio of total tree height that is trunk (no branches) – because it is activated only in those grid cells with forest (i.e., vegetation class with overstory, spanning 22% of our study domain) as land cover type. Finally, we found five mutually related soil parameters that do not allow independent variations: soil bulk density (*bd*); soil particle density (*sd*); fractional soil moisture content at the critical point (θ_{cr}), fractional soil moisture content at the wilting point (θ_{wp}) and residual soil moisture (θ_r). These parameters are related following:

$$\theta_{cr} \geq \theta_{wp} \geq \frac{\theta_r}{\left(1 - \frac{bd}{sd}\right)} \quad (1)$$

From these five parameters, we only include θ_r and bd because (1) perturbing its values did not affect numerical solutions, and (2) Bennett et al. (2018) included θ_{cr}, θ_{wp}, bd and sd in their sensitivity analysis, showing that these parameters did not have substantial effects on model simulations. Finally, those parameters that showed little or no sensitivity in the initial phases of the study were purposely discarded.

Table 3. Parameters of the VIC model considered in this study.

Parameter	Description	Units	Min	Max	Comment
Soil parameters					
INFILT	Variable infiltration curve parameter	-	0.001	0.4	Based on Mendoza et al. (2015b)
Ds MAX	Maximum velocity of baseflow	mm/d	1	50	Based on Melsen et al., (2016)
Ds	Fraction of Ds_{max} where non-linear baseflow occurs	-	0.00005	1	Based on Mendoza et al. (2015b)
Ws	Fraction of maximum soil moisture where non-linear baseflow occurs	-	0.0009	1	Based on Mendoza et al. (2015b)
c	Exponent used in baseflow curve	-	1	4	Based on Melsen et al. (2016)
$EXPT_i$	Exponent in Campbell's equation for hydraulic conductivity of soil layer i	-	5	30	Based on Melsen et al. (2016)
$Ksat_i$	Saturated hydraulic conductivity of soil layer i	mm/d	1	10000	Based on Demaria et al. (2007)
$Depth_1$	Thickness of layer 1 (uppermost)	m	0.01	0.5	Based on Demaria et al. (2007)

Parameter	Description	Units	Min	Max	Comment
$Depth_2$	Thickness of layer 2	m	$Depth_1 + 0.1$	$Depth_1 + 4$	Based on Melsen et al. (2016)
$Depth_3$	Thickness of layer 3 (lowermost)	m	0.1	4	Based on Melsen et al. (2016)
dp	Soil thermal damping depth	m	1	3.75	Based on Gates & Evans (1964) and Al Nakshabandi & Kohnke (1965)
$quartz_i$	Quartz content of soil layer i	-	0.1	0.82	Based on Hogue et al. (2005) and Rosero et al. (2010)
bulk $density_i$	Bulk density of layer i	kg/m^3	1200	1609	Based on Cosby et al. (1984); Rawls et al. (1992) and Reynolds et al. (2000)
rough	Surface roughness of bare soil	m	0.0001	0.08	Based on Woodward (1999)
Z0_SNOW	Surface roughness of snowpack	m	0.0001	0.01	Based on range suggested by Marks & Dozier (1992) and Reba et al. (2014)
Resid moist	Residual soil moisture of layer i	-	0.02	0.109	Based on Rawls et al. (1992)
Vegetation parameters					
rarc	Architectural resistance of vegetation type	s/m	2	50	Based on Ducoudré et al. (1993)
rmin	Minimum stomatal resistance of vegetation type	s/m	30	300	Based on Melsen et al. (2016)
LAI*	Leaf-area index of vegetation type	-	**0.1**	**1.16**	Multipliers obtained from leaf-area index range 0.01-7 based on Dorman & Sellers (1989) and Myneni et al. (1997)
ALB*	Shortwave albedo for vegetation type	-	**1**	**1.65**	Multiplier obtained from shortwave albedo range 0.1-0.33 based on Dorman & Sellers (1989)
ROU*	Vegetation roughness length	-	**0.82**	**2.11**	Multiplier obtained from roughness length range 0.06-2.6 m based on Dorman & Sellers (1989)
DIS*	Vegetation displacement height	-	**0.82**	**2.11**	Multiplier obtained from roughness length range 0.06-2.6 m based on Dorman & Sellers (1989) and VIC definitions
Root depth i	Root zone thickness (sum of depths is total depth of root penetration) of layer i	m	0.1	3	Based on Melsen et al. (2016)
Root fraction i	Fraction of root in the current root zone of layer i.	-	0	1	Based on Bohn & Vivoni (2016)
Snow and general parameters					
Tmin	Minimum temperature at which rain can fall.	°C	-1.5	0	Based on Melsen et al. (2016)

Parameter	Description	Units	Min	Max	Comment
Tmax	Maximum temperature at which snow can fall.	°C	Tmin + 0.5	Tmin + 1.5	Based on Melsen et al. (2016)
NEWALB	New snow albedo	-	0.7	0.99	Based on Mendoza et al. (2015b)
ALBAA	Base in snow albedo function (accumulation)	-	0.88	0.99	Based on Mendoza et al. (2015b)
ALBTHA	Base in snow albedo function (melt)	-	0.66	0.98	Based on Mendoza et al. (2015b)

*This parameter is temporally distributed (monthly variations) and, therefore, its sensitivity is analyzed based on multipliers. Although description and units refer to actual parameters of VIC, parameter values in bold represent the multiplier values (instead of actual parameters).

3.3 Sensitivity analysis approach

We used the Distributed Evaluation of Local Sensitivity Analysis (DELSA; Rakovec et al., 2014) method, which is a derivative-based, hybrid local-global approach. DELSA combines elements from the method of Morris (Morris, 1991), the Sobol' method (Sobol', 2001) and regional sensitivity analysis (Hornberger and Spear, 1981), and provides robust results with a fewer number of model simulations compared to variance-based global methods such as Sobol'. Although our implementation only examines first-order sensitivities (as in Mendoza et al., 2015b; Zegers et al., 2020; among other studies) DELSA has unexplored potential to quantify parameter interactions, which could be achieved by including additional terms in the local total variance (Sobol' and Kucherenko, 2010).

Consider a transformation f and a vector θ with k parameters, which provides a metric Ψ describing model output:

$$\Psi = f(\theta), \quad f: R^k \rightarrow R \tag{2}$$

Given a sample point θ^* in the parameter space, the gradient for metric Ψ and parameter θ_j around this point - i.e., $\frac{\partial \Psi}{\partial \theta_j}|_{\theta^*}$ - is considered a measure of local sensitivity. In this work, we follow Rakovec et al. (2014) and compute such gradient using a forward, finite difference approach with 1% change in the parameter value:

$$\frac{\partial \Psi}{\partial \theta_j}|_{\theta^*} = \frac{\Psi(\theta_j^* + 0.01\theta_j^*) - \Psi(\theta_j^*)}{0.01\theta_j^*} \tag{3}$$

In equation (3), $\Psi(\theta^*)$ is a signature measure of hydrologic behavior, formulated by contrasting model output at the point θ^* with that obtained from a reference parameter set θ^{ref} in the grid cell of interest (see section 3.3.2 for details). The first-order sensitivity measure for the j^{th} parameter is calculated at each sample point as:

$$S_j^L = \frac{\left(\frac{\partial \Psi}{\partial \theta_j}|_{\theta^*}\right)^2 s_j^2}{V_L(\theta^*)} \tag{4}$$

Where s_j^2 is the a priori parameter variance of the j^{th} parameter, and $V_L(\theta^*)$ is the linearized local variance:

$$V_L(\theta^*) = \sum_{j=1}^{k} \left(\frac{\partial \Psi}{\partial \theta_j} |_{\theta^*} \right)^2 s_j^2 \quad (5)$$

Finally, s_j^2 is obtained from the variance of a uniform distribution (Rakovec et al., 2014), which is $\frac{1}{12}\left(\theta_{j,max} - \theta_{j,min}\right)^2$.

The first-order sensitivity indices vary between 0 and 1, and the sum of first-order sensitivities from all parameters at each sampling point is equal to 1. Local sensitivities can be examined through their cumulative frequency distribution across the parameter space, or by computing a specific statistical property. Here, we quantify the relative contribution of a specific parameter using the area above the curve of the full frequency distribution:

$$IS_j^L = 1 - \int_0^1 F\left(S_j^L\right) dS_j^L \quad (6)$$

3.4 Performance metrics

We use eight model evaluation metrics to characterize the sensitivity of simulated hydrological processes to variations in model parameters. The notation, brief description, mathematical formulation, and physical process associated with each metric are detailed in Table 4. These metrics are computed by contrasting model output from sampling points produced for DELSA, with a reference, national scale dataset with simulated states and fluxes obtained from the National Water Balance database (DGA, 2018, 2019, 2020) for the historical period 1985-2015. Such dataset was developed by running the VIC model at the same grid discretization employed here (i.e., 0.05°x0.05°), using a combination of CR2MET version 2.0, ERA-Interim and ERA5 output as meteorological forcings. The spatially distributed parameter fields for our reference simulation were developed via parameter regionalization, based on the similarity between possible donor catchments – whose parameters were calibrated individually (Vásquez et al., 2021) – and each grid cell across the domain, following Beck et al. (2016). The reader is referred to Vásquez et al., (2021) and DGA (2018, 2019, 2020; in spanish) for more details on individual model calibration and parameter regionalization procedures used to generate the reference simulation.

Four evaluation metrics are formulated from runoff time series. The first objective function is the root-mean-square error (RMSE), which is a standard metric that emphasizes high flows. The second metric selected is the transformed-root-mean-square error (TRMSE), for which the simulated and observed runoff time series are transformed using a Box-Cox transformation to emphasize low flows (Misirli et al., 2003). The third objective function is the flow duration curve (FDC) midsegment slope error (FMS). The midsegment slope of this curve represents the variability, or flashiness, of the flow magnitudes, so it measures how well a model captures the distribution of the mid-level flows. A steep slope of the FDC indicates flashiness of the streamflow response, whereas a flatter curve indicates a relatively damped response and a higher storage (Casper et al., 2012; Yadav et al., 2007). The fourth evaluation metric is the runoff ratio error (RR), considered as a measure of the general water balance and, therefore, as a signature of the evapotranspiration model component (Mendoza et al., 2015b).

Table 4. Parameter sensitivity metrics used in this study.

Notations	Short descriptions	Formulas	Indicator of processes
RMSE	Root-mean-squared-error	$\sqrt{\frac{1}{N}\sum_{t=1}^{N}\left(Q_t^{sim}-Q_t^{ref}\right)^2}$	High flows
TRMSE	Transformed-root-mean-squared-error	$\sqrt{\frac{1}{N}\sum_{t=1}^{N}\left(Z_t^{sim}-Z_t^{ref}\right)^2}$ $Z_t=\frac{(1+Q_t)^{\lambda}-1}{\lambda};\ \lambda=0.3$	Low flows
FMS	Flow duration curve midsegment slope error	$\left\lvert\frac{Q_{m_1}^{sim}-Q_{m_2}^{ref}}{m_1-m_2}-\frac{Q_{m_1}^{obs}-Q_{m_2}^{ref}}{m_1-m_2}\right\rvert$	Variability, or flashiness, of the flow magnitudes
RR	Runnof ratio error	$\left\lvert\frac{R_{sim}}{P_{sim}}-\frac{R_{ref}}{P_{ref}}\right\rvert$	Overall water balance (ET processes)
PeakSWE	Peak SWE error	$\lvert max\{SWE_t\}_{sim}-max\{SWE_t\}_{ref}\rvert$	Maximum long-term SWE accumulation
SnowLength	Snow length error	$\left\lvert\sum days \in SWE_{sim}>x-\sum days \in SWE_{ref}>x\right\rvert$ $x=1\ mm$	The number of days when snow is on the ground
SUBL	Sublimation error	$\lvert Subl_{sim}-Subl_{ref}\rvert$	Mean error on sublimation estimation
TRANSP	Transpiration error	$\lvert Transp_{sim}-Transp_{ref}\rvert$	Mean error on transpiration estimation

N, number of time steps; Q_t, flow for time step t; Z_t, flow transformed for time step t; Q_{m_1}, m_1 percentile flow of simulated flow duration curve; $m_1=70$; Q_{m_2}, m_2 percentile flow of simulated flow duration curve; $m_2=30$; R, grid-averaged mean annual runnof; P, grid-averaged mean annual precipitation; SWE_t, Snow water equivalent for time step t; Subl, grid-averaged mean annual sublimation; Transp, grid-averaged mean annual transpiration.

We use two metrics to characterize snow cover processes: the error in long-term simulated peak SWE, and the error in snow cover duration, quantified by the number of days with snow on the ground (Mizukami et al., 2014). Finally, we include two metrics based on evaporation fluxes. The sublimation error (SUBL) emphasizes the net sublimation from the snowpack surface, and the plant transpiration error (TRANSP).

3.5 Experimental setup

We apply the DELSA method in 5,574 grid cells across continental Chile, which are contained within the 101 catchments described in section 2. In each grid cell, hydrologic model simulations are conducted at 3-hourly time steps for a 12-year period (April/1999 – March/2011), with the first two years used as the spin-up period. The model is run in full energy balance mode, which means that both energy and water balances are solved, and 3-hourly outputs are aggregated to daily time steps for subsequent analyses.

In this study, we use the Latin hypercube sampling (LHS) method to obtain 200 sample points across the parameter space, for which first-order sensitivity indices are computed. LHS is an efficient simulation technique, and especially suitable for statistical and sensitivity calculations (Vořechovský, 2015). To stratify the parameter space, we sample uniformly in a 43-dimensional hypercube, and map onto the parameter space using the inverse cumulative distribution function of each parameter's prior. Since DELSA is used here, all parameter distribution functions are assumed to be uniform. The computational cost of applying DELSA at each cell is N_l (k +1) = 8,800 model runs, where N_l is the number of sample points (200) and k is the number of parameters (43), and the total number of models runs required for this study is 49,051,200.

In this paper, a parameter is considered redundant or insensitive when the median value of integrated first-order sensitivity indices across all grid cells is smaller than 0.05 for at least seven of the eight evaluation metrics listed in Table 4. Parameter sensitivity results are also examined per metric (section 3.4) and grid cell climate type based on the aridity index (UNEP, 1997; Verbist et al., 2010; Table 5).

Finally, we use the Spearman rank correlation coefficient, r_s, to measure the degree of association between parameter sensitivities and physiographic/hydroclimatic characteristics listed in Table 2. These attributes were chosen due to their ability to improve the prediction of hydrological signatures (Addor et al. 2018) and because they are relatively easy to obtain.

Table 5. Climate classification used to group model grid cells.

Classification	Humid	Humid sub-humid	Dry sub-humid	Semi-arid	Arid	Hyper arid
Aridity index	<1	1 to 1.53	1.53 to 2	2 to 5	5 to 20	>20
Number of grid cells	2189	772	318	992	803	499

4 Results and discussion

4.1 Intra and inter-basin variability in parameter sensitivities

Figure 3 shows the cumulative distribution function of sensitivity indices S_j^L for different grid cells and combinations of signature measure and parameter. Figure 3a compares the results obtained for grid cells from hydroclimatically different basins – from arid to humid – showing high parametric sensitivities for RMSE-*INFILT* in basins located in the north zone (arid regime) and low sensitivities to those of the central-south zone, while the opposite is observed for TRMSE - *DsMAX*. Such dependence between hydroclimatic characteristics of the basin and parameter sensitivities was also reported by Demaria et al. (2007). Gou et al. (2020) also found that sensitivities were strongly related to environmental characteristics, including climate, vegetation, soil and topographic features. Figure 3b illustrates the intra-catchment variability in parameter sensitivities for a basin with wet climate (8317001; Biobio River at Rucalhue). One can note that, for some metric-parameter combinations (i.e., SUBL-*Z0_SNOW*), there are large spatial variations related to grid cell location while, for others (i.e., FMS-*Ds*), intra-catchment differences between the CDFs are very small.

To further illustrate intra-basin differences in parameter sensitivities, Figure 4 and Figure 5 show the spatial distribution of the IS_j^L indices for the leaf area index (*LAI*) and the snow albedo

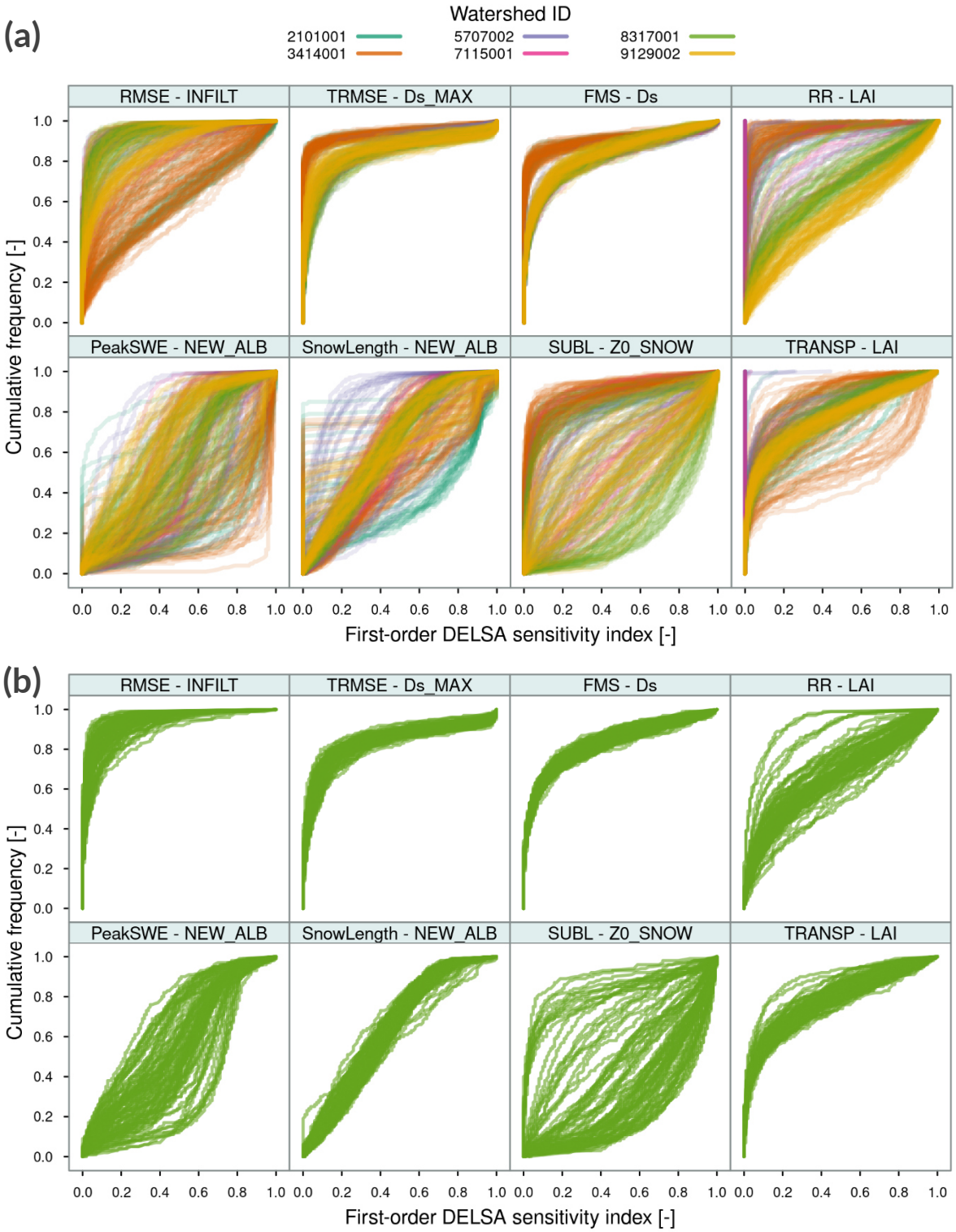

Figure 3. Comparison of cumulative frequency distributions of first-order DELSA indices for the most sensitive parameters associated with each evaluation metric. The most sensitive parameter was determined based on the median sensitivity index IS_j^L from all grid cells. (a) Comparison between grid cells from six hydroclimatically different basins (shown in Figure 2). (b) Comparison grid cells selected from the same basin 8317001 (Biobio River at Rucalhue).

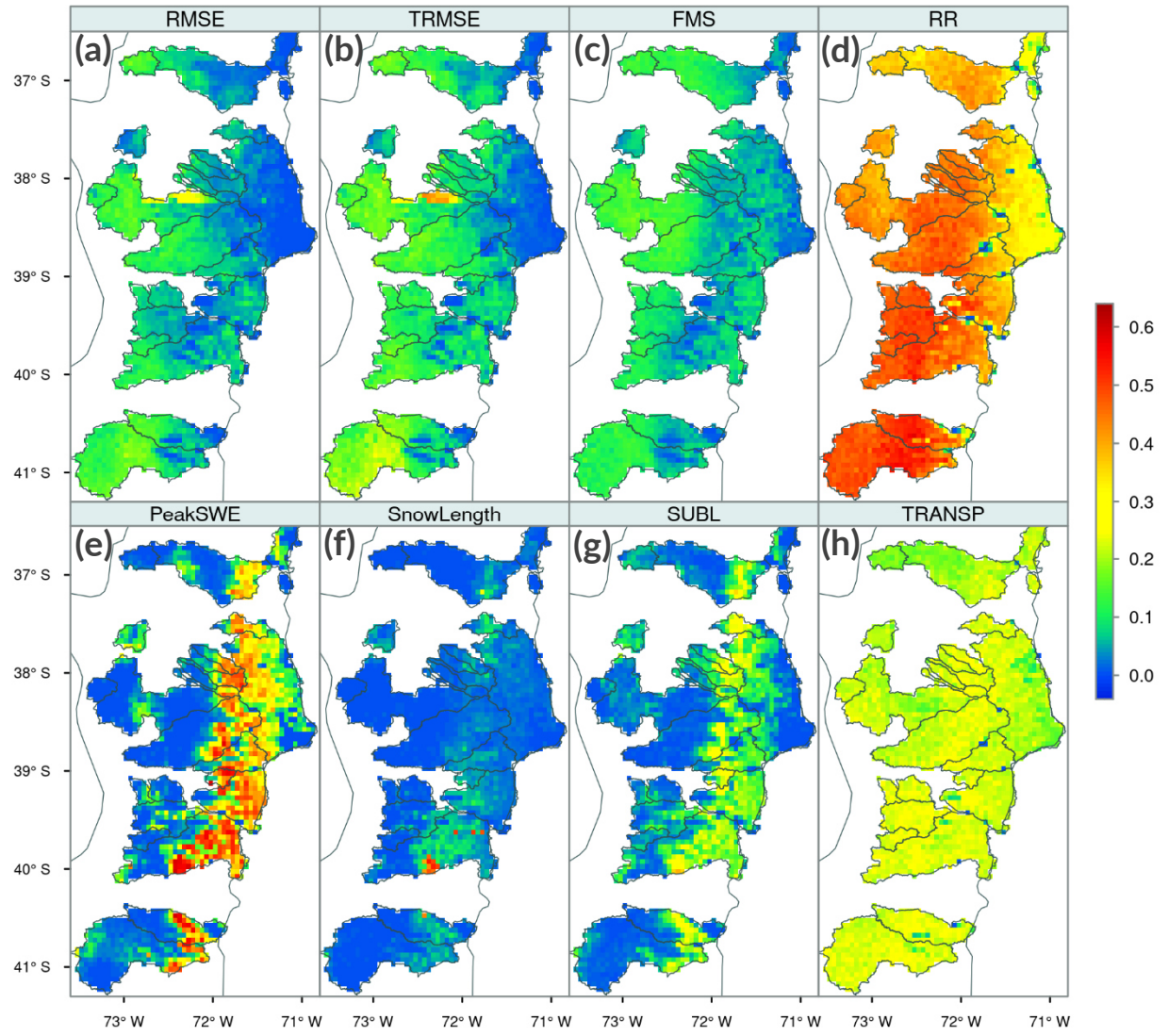

Figure 4. Spatial distribution of integrated first-order DELSA sensitivity indices for the leaf area index (*LAI*) across a humid subdomain located in Southern Chile. Results are displayed for eight sensitivity metrics: (a) RMSE, (b) TRMSE; (c) FMS; (d) RR; (e) PeakSWE; (f) SnowLength; (g) SUBL; (h) TRANSP.

parameter *ALBTHA*, respectively, over a cluster of sub-humid and humid basins located in southern Chile. For the *LAI* parameter (Figure 4), a west-east gradient in IS_j^L is observed for RMSE (high flows), TRMSE (low flows) and FMS (flashiness of runoff), with increasing sensitivity to *LAI* variations towards the coast, while an inverse pattern is observed for the same metrics and *ALBTHA* (i.e., larger sensitivities towards the Andes, Figure 5). For PeakSWE, SUBL, and – to a smaller degree – SnowLength, *LAI* yields larger sensitivities in vegetated areas where snow accumulates during winter (Figure 4), matching those locations where forest is the dominant land cover type, which is also the only vegetation class with overstory (e.g. trees). Notably, very large variations in PeakSWE sensitivities to *LAI* are observed over relatively short distances due to differences among grid cells in the fraction of land cover defined as forest. Figure 4 also shows

that *LAI* does not yield a clear sensitivity pattern in RR and TRANSP throughout this subdomain, although IS_j^L values are higher for RR. For this metric, there are spatial singularities where the sensitivity is minimal or null since, in these areas, the fraction of ground cover defined as bare soil increases considerably, even reaching a 100% of bare soil (LAI ~ 0) for some cells.

The results presented in Figure 5 reinforce the idea that hard-coded parameters should be exposed to users (Cuntz et al., 2016; Mendoza et al., 2015a). In particular, Figure 5 shows the large effects of *ALBTHA* variations on SnowLength (with a very pronounced east-west gradient) and, to a smaller degree, on PeakSWE and SUBL. *ALBTHA* also affects runoff-based metrics along the Andes, especially on simulated high (RMSE) and low (TRMSE) flows.

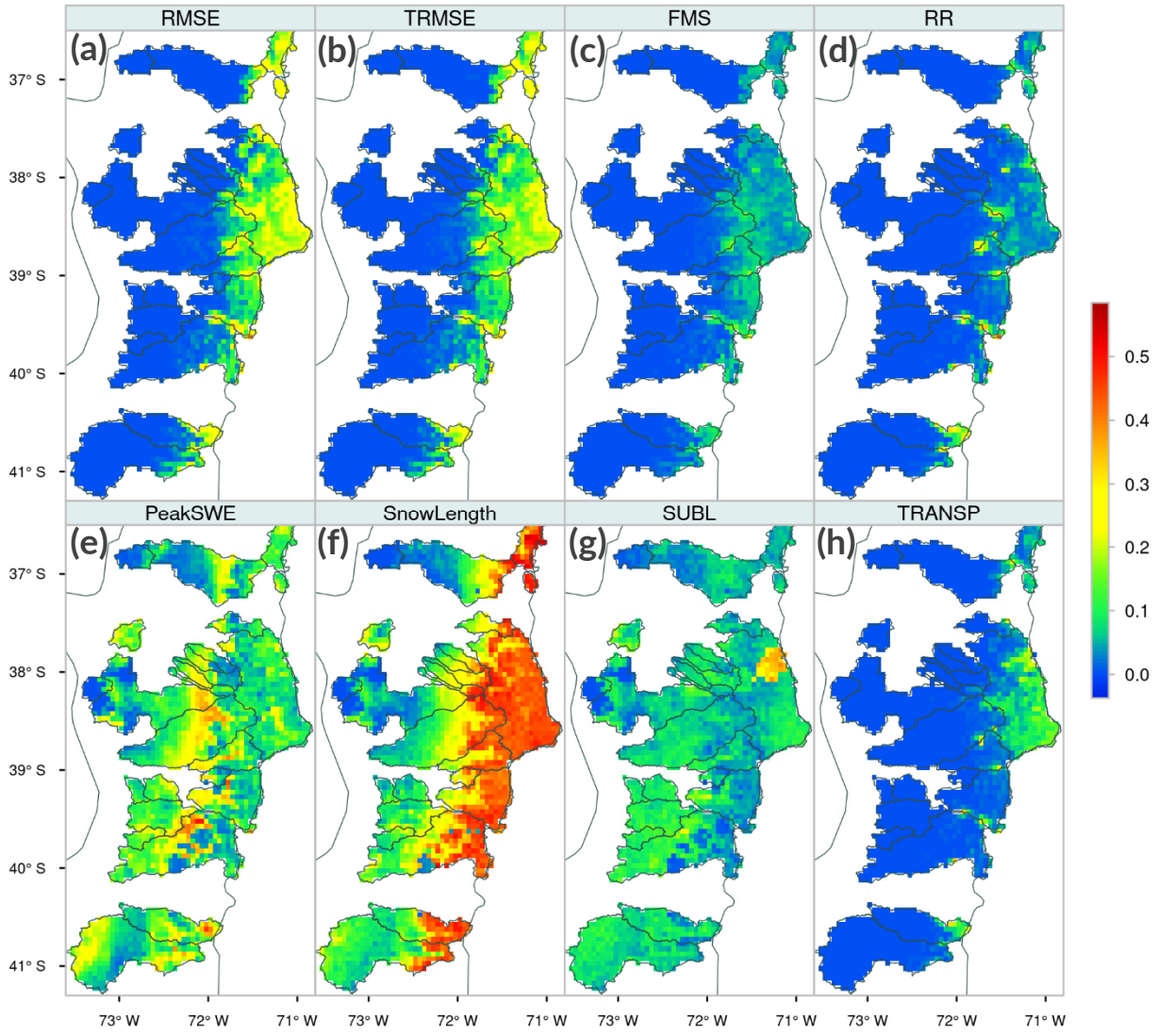

Figure 5. Same as in Figure 4, but for the base in the snow albedo function *ALBTHA* (melt).

4.2 Identification of most sensitive parameters

Figure 6 displays box plots comprising IS_j^L results from all grid cells in the study domain, for each parameter and evaluation metric (displayed in different panels). The results show that 72% of the parameters analyzed (i.e., 31) yield little sensitivities for the metrics examined here. Conversely, a suite of 12 sensitive parameters are associated to soil (*INFILT*, *Ds*, *DsMAX*, *Ws*, *Expt2*, *Depth2*, *Depth3*), snow (*NEWALB*, *ALBTHA*, and *ALBAA*), and vegetation (*Rmin* and *LAI*) processes. Figure 7 shows the spatial variation of IS_j^L for the 12 parameters identified as the most sensitive across the 101 basins of continental Chile.

For the case of high flows (RMSE), low flows (TRMSE), and flashiness of runoff (FMS), the parameters identified as sensitive are *INFILT*, *Ds*, *DsMAX*, *Ws*, *Expt2*, *Depth2*, and *Depth3* (see top three panels in Figure 6). The parameter *INFILT* controls the shape of the variable infiltration capacity curve (Wood et al., 1992; Zhao et al., 1980), and thus the partitioning of rainfall or snowmelt into infiltration and surface runoff. A higher *INFILT* value yields less infiltration and higher surface runoff. The RMSE and TRMSE metrics are particularly sensitive to *INFILT*, indicating a key role in the generation and timing of high and low flows. This parameter has been identified as sensitive in all the studies listed in Table 1.

DsMAX is the maximum velocity of baseflow; *Ds* and *Ws* are the fractions of *DsMAX* and the fraction of the maximum soil moisture content in the third layer, respectively, where non-linear baseflow occurs. These three parameters are involved in the Arno formulation of subsurface runoff (Franchini and Pacciani, 1991; Todini, 1996), controlling the speed of baseflow release from the third soil layer (Liang et al., 1994) and, specifically, the non-linear part of the baseflow generation function. The sensitivity indices found here for these parameters are consistent with the high sensitivity measures reported by Mendoza et al. (2015b), Melsen et al. (2016) and Wi et al. (2017).

The *Expt2* parameter is an exponent of the Brooks-Corey relationship (Brooks and Corey, 1964) and controls the hydraulic conductivity between the second and third soil layers. A small value for the *Expt2* parameter increases inter-layer drainage for the same soil moisture content, and therefore increases baseflow generation. The *Depth2* parameter is the thickness of the second soil layer. In general, thicker soil layers slow seasonal peak flows and increase water loss due to evapotranspiration (Xie et al., 2007). It should be noted that the parameter *Depth2* has been identified as highly sensitive by many authors (Demaria et al., 2007; Gou et al., 2020; Lilhare et al., 2020; Mendoza et al., 2015b; Wi et al., 2017; Yeste et al., 2020). Finally, *Depth3* is the thickness of the third layer of soil, and the large sensitivities obtained here agree with the results reported by Mendoza et al. (2015b) and Wi et al. (2017).

The results in Figure 6 show that *Expt2* and *Depth2* also provide large sensitivities for metrics focused on evaporative fluxes (i.e., RR and TRANSP). Other parameters that are relevant for these processes are *LAI* and the minimum stomatal resistance (*Rmin*). Indeed, Chaney et al. (2015) reported high sensitivity of *Rmin* for annual flow biases. *LAI* is a dimensionless quantity that characterizes intra-annual variations in plant canopies, and it is defined as the one-sided green leaf area per unit ground surface area. On the other hand, *Rmin* is one of the parameters that control canopy resistance when estimating transpiration from each vegetation class, following the formulations proposed by Blondin (1991) and Ducoudré et al. (1993). Both *LAI* and *Rmin* provide null sensitivities if the land cover type is bare ground; however, *Rmin* can also produce null sensitivities in vegetated grid cells.

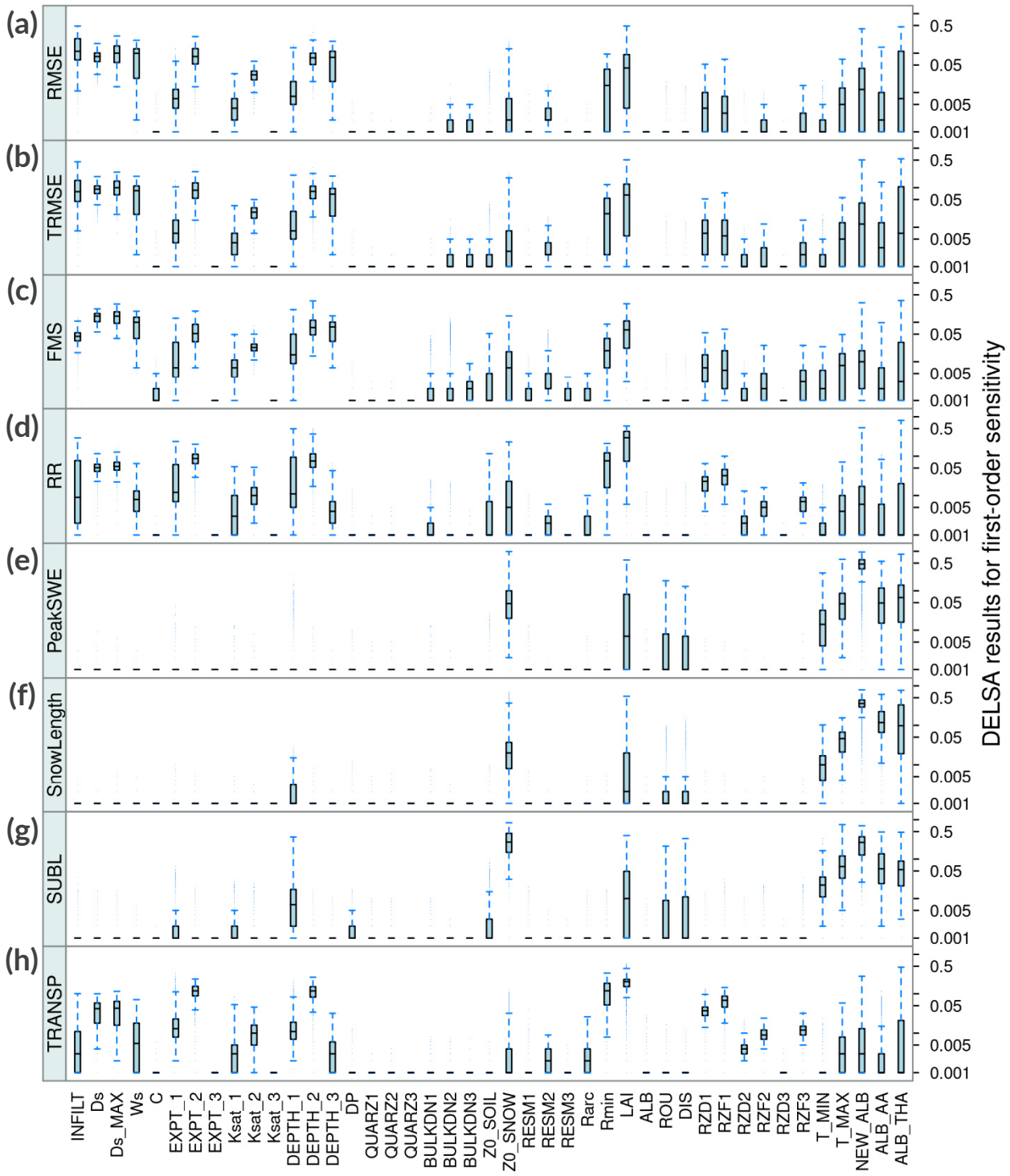

Figure 6. Boxplots comprising integrated first-order DELSA sensitivity indices from all modeling units (5,574 grid cells). Results are displayed for all parameters (x-axis) and sensitivity metrics which are presented in different panels: (a) RMSE, (b) TRMSE; (c) FMS; (d) RR; (e) PeakSWE; (f) SnowLength; (g) SUBL; (h) TRANSP.

Figure 6 reveals the large influence of hard-coded parameters on PeakSWE, SnowLegth and SUBLM, in particular *NEWALB*, *ALBTHA* and *ALBAA*. The *NEWALB* parameter is the new snow surface albedo, which controls the reflection of solar radiation and, therefore, the energy exchange between the atmosphere, forest canopy and the surface layer of the snowpack (Andreadis et al., 2009). Additionally. The *ALBAA* and *ALBTHA* parameters represent the albedo decay in the accumulation and melting season in the snow albedo curve, respectively (USACE, 1956). These seasons are defined based on the absence or presence of liquid water in the surface snow cover, respectively. These results correspond well with the high sensitivities reported by Mendoza et al. (2015b) for these three hard-coded parameters. Finally, the snow surface roughness length (*Z0_SNOW*) also affects sublimation rates across Andean subdomains.

Table 6 lists, for each evaluation metric (i.e., physical process to be represented) and climatic zone (using the classification from Table 5), the three most important parameters**.**

Table 6. Summary with the most sensitive VIC parameters found for each metric (rows) and climatic type. The three most important parameters are determined based on the median of integrated first-order DELSA sensitivity indices and are sorted by ranking (i.e., 1st, 2nd, and 3rd most sensitive).

Classification	Humid	Humid sub-humid	Dry sub-humid	Semi-arid	Arid	Hyper arid
RMSE	Ds_MAX Ws DEPTH_3	Ds_MAX Ws DEPTH_3	INFILT Ws Ds_MAX	INFILT EXPT_2 DEPTH_2	INFILT EXPT_2 DEPTH_2	INFILT EXPT_2 DEPTH_2
TRMSE	Ds_MAX Ws Ds	LAI Ds_MAX Ds	LAI DEPTH_2 Ds	INFILT DEPTH_2 EXPT_2	INFILT EXPT_2 DEPTH_2	INFILT EXPT_2 DEPTH_2
FMS	Ds_MAX Ds Ws	Ds Ds_MAX LAI	Ds Ds_MAX LAI	Ds Ds_MAX DEPTH_2	DEPTH_2 EXPT_2 Ds	DEPTH_2 EXPT_2 Ds
RR	LAI Rmin EXPT_2	LAI Rmin EXPT_2	LAI EXPT_2 DEPTH_2	LAI EXPT_2 DEPTH_2	INFILT DEPTH_1 EXPT_2	DEPTH_2 INFILT DEPTH_1
PeakSWE	NEW_ALB ALB_THA LAI	NEW_ALB ALB_THA ALB_AA	NEW_ALB Z0_SNOW ALB_THA	NEW_ALB ALB_AA T_MAX	NEW_ALB ALB_AA Z0_SNOW	NEW_ALB ALB_AA Z0_SNOW
SnowLength	NEW_ALB ALB_THA ALB_AA	NEW_ALB ALB_AA ALB_THA	NEW_ALB ALB_AA ALB_THA	NEW_ALB ALB_AA T_MAX	NEW_ALB ALB_AA ALB_THA	NEW_ALB ALB_AA Z0_SNOW
SUBL	ZO_SNOW NEW_ALB ALB_THA	NEW_ALB Z0_SNOW T_MAX	Z0_SNOW NEW_ALB T_MAX	NEW_ALB Z0_SNOW ALB_AA	NEW_ALB Z0_SNOW ALB_AA	NEW_ALB ALB_AA Z0_SNOW
TRANSP	LAI Rmin EXPT_2	LAI Rmin DEPTH_2	LAI DEPTH_2 EXPT_2	LAI DEPTH_2 EXPT_2	EXPT_2 LAI DEPTH_2	EXPT_2 DEPTH_2 LAI

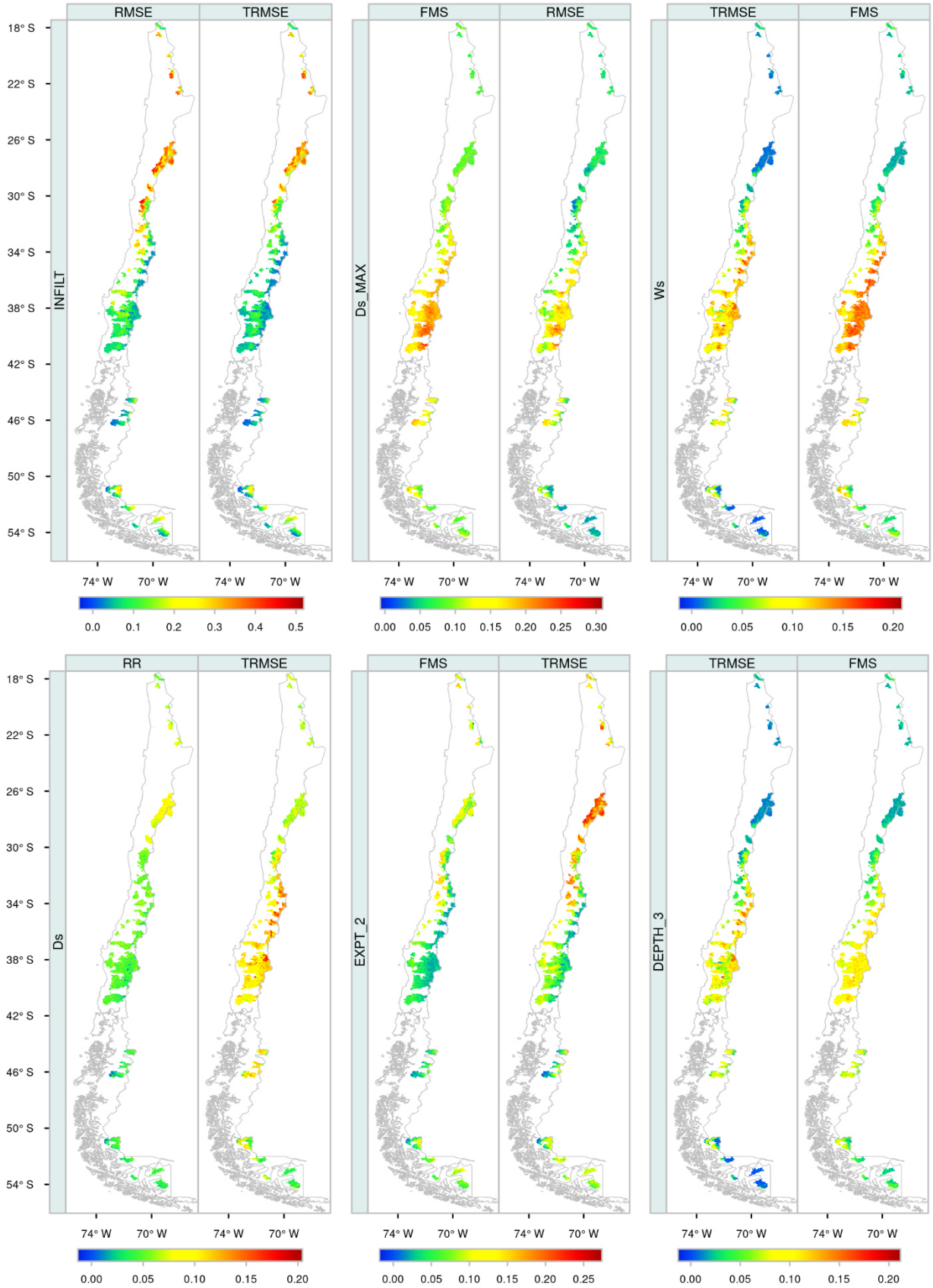

Figure 7. Integrated first-order DELSA sensitivity indices for all grid cells within our study basins. The results are displayed only the 12 most sensitive parameters, and their associated most impacted metrics.

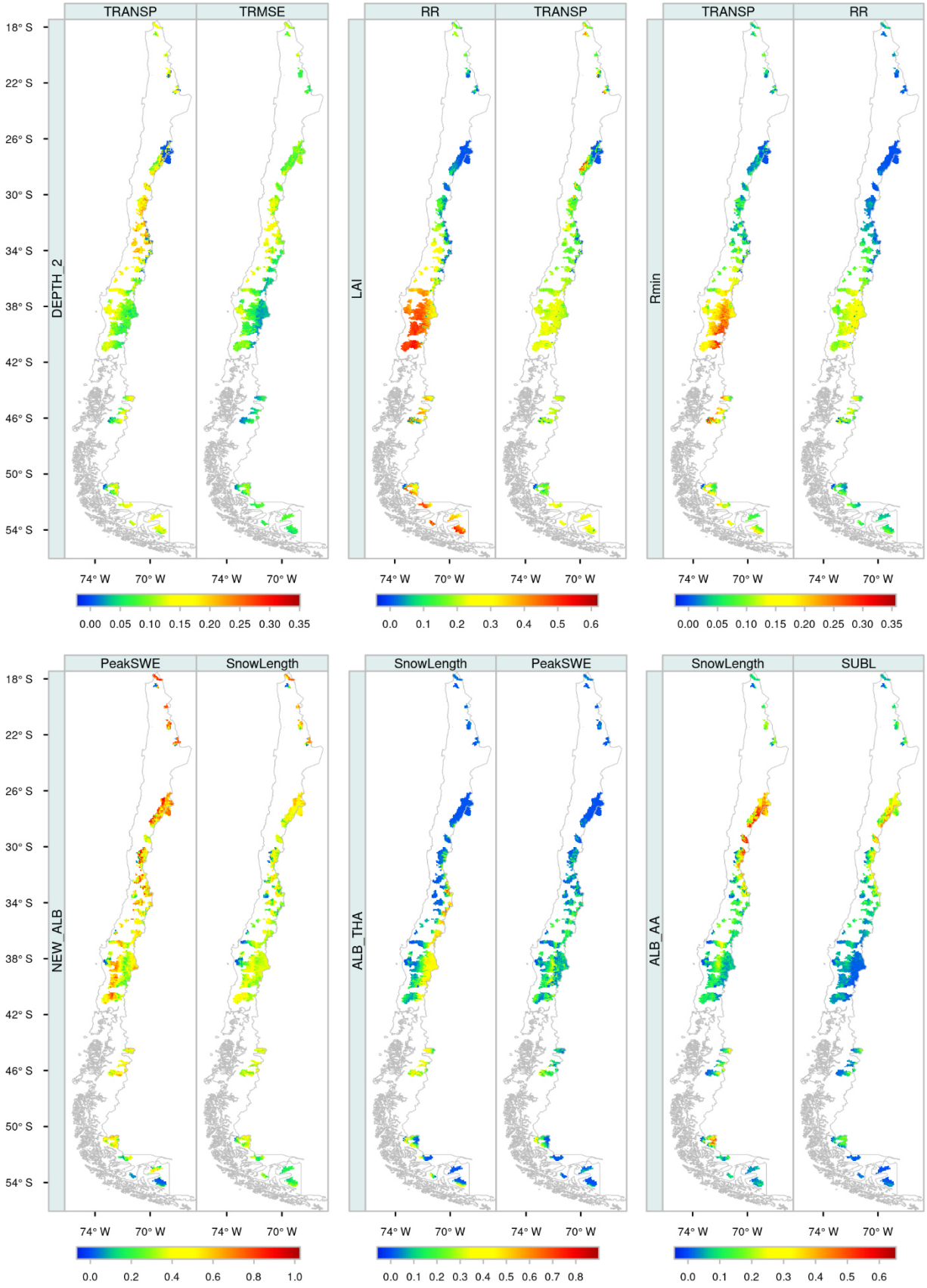

Figure 7. (continued).

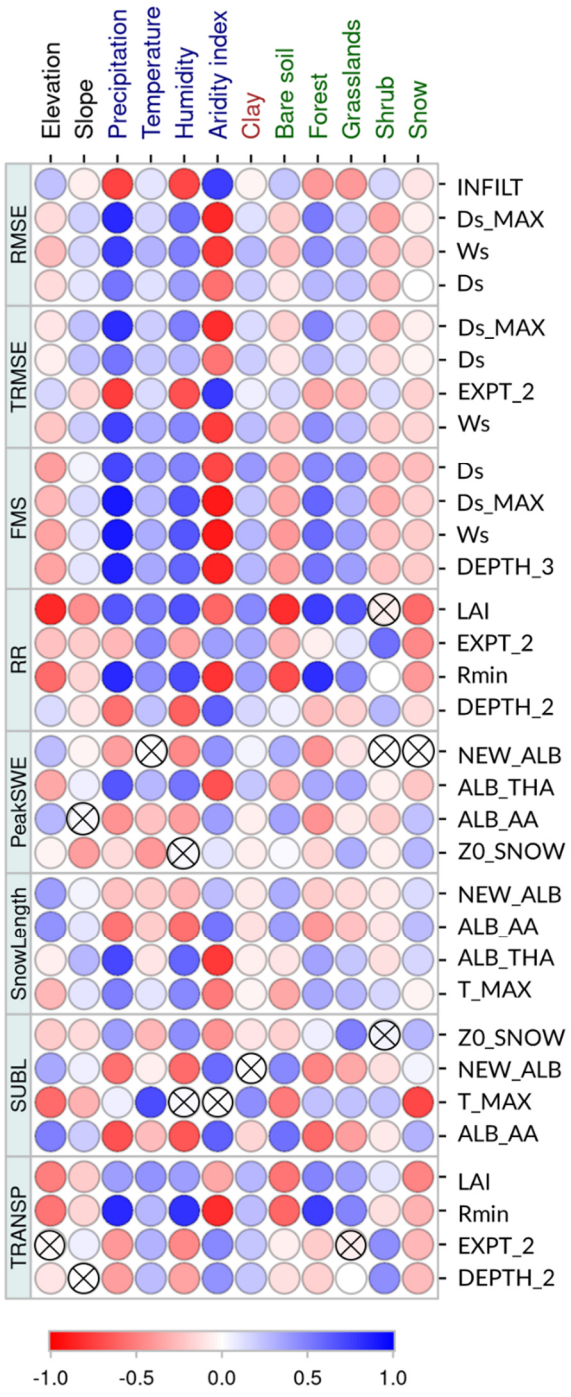

Figure 8. Spearman rank correlation coefficient between integrated first-order DELSA sensitivity indices and grid cell characteristics. Results are displayed only for the 4 most sensitive parameters affecting each metric. The crosses indicate correlation values whose p-values are lower than 0.05.

4.3 What drives parameter sensitivities across continental Chile?

Figure 8 shows the Spearman rank correlation coefficient, r_s, between parameter sensitivities and a suite of climatic, topographic, land cover and soil-related grid cell attributes detailed on Table 2. The results show that the strength of the signal varies depending on the combination of metric and parameter, with the maximum correlations generally found for soil parameters, such as *DsMAX* and *Ws* with precipitation ($r_s = 0.91$) and aridity index ($r_s = -0.91$) for the FMS function (flashiness of the flow). Conversely, the minimum correlations are found for snow parameters.

The results in Figure 8 also indicate that high correlations (either positive or negative) are mainly associated with climate indices, which exert a stronger influence compared to the remaining attribute classes. These high correlations are somewhat expected, because some combinations of hydrological signatures and parameters inherit strong spatial climate patterns (Addor et al. 2018) – compare, for example, aridity index Figure 1(d) with panel *DsMAX* – FMS; RMSE in Figure 7.

Among climate descriptors, the aridity index, mean annual precipitation and relative humidity yield the highest correlations. Conversely, temperature exhibits a weak influence on parametric sensitivity. The lowest correlations are obtained for mean slope (topographic attribute), shrub fraction (land cover attribute) and mean clay content of soil (soil attribute). The key influence of climatic conditions on hydrological behavior is not new. Aridity is commonly regarded as the main driver of water partitioning at the land surface (Budyko, 1974; Hrachowitz et al., 2013).

Figure 8 shows that the extent to which parametric sensitivities are related to grid cell attributes depends on the target evaluation metric (i.e., runoff, evaporative processes and snow processes), with three distinct groups containing the same influential parameters. In the following subsections, we discuss the results based on these groups, with emphasis on spatial patterns and process interpretation across our study basins.

4.3.1 Runoff-oriented metrics

The results presented in Figure 7 (see RMSE and TRMSE) and Figure 8 (RMSE) show a direct relationship between the sensitivities provided by *INFILT*, and the degree of aridity, especially in semi-arid to hyper-arid subdomains. The runoff-oriented metrics are also sensitive to baseflow generation parameters *Ds*, *Ws* and *DsMAX* in most basins – with a similar spatial distribution of IS_j^L values –, excepting those located in the north and some areas in Southern Patagonia, where climatic conditions are arid or hyper-arid. In basins located in the extreme north, small sensitivities can be attributed to local climate characteristics: most precipitation events in that area occur in summer (i.e., December-March) due to orographic rains caused by air masses coming from the Amazon region, and there is usually little recharge to the aquifers. Additionally, the third soil layer in these basins generally does not reach saturation; therefore, runoff simulations in those areas are insensitive to variations in *Ds* and *Ws* because the non-linear part of the baseflow function is only activated when the moisture storage in the third layer exceeds a threshold (Gou et al., 2020). Because of the dependency of *DsMAX* with precipitation, this parameter could be playing a key role in baseflow generation processes over Andean regions (Figure 7). Finally, a similar spatial distribution of integrated first-order sensitivities for *Ds*, *Ws* and *DsMAX* is expected, since they all focus on baseflow generation (see panels *DsMAX* - FMS, RMSE -; *Ws* -TRMSE, FMS-; *Ds* - TRMSE- in Figure 7).

Expt2 is identified as sensitive for runoff-oriented metrics in basins with semi-arid to hyper-arid climates, characterized by small annual precipitation amounts and permanent water stress. In these hydroclimatic regimes, there is usually not enough water to reach the third soil layer, so water is stored in the second layer and drainage is mainly controlled by *Expt2*, affecting the vertical redistribution of soil moisture (FMS) and low flows (TRMSE), as shown in Figure 7. *Depth2* provides large runoff sensitivities in dry-subhumid to hyper-arid hydroclimatic regimes, for the same reasons as *Expt2*. Variations in the depth of the second soil layer produce changes in the water content, and higher (lower) values of *Depth2* at the same water content produce lower (higher) soil moisture content, affecting drainage between soil layers.

Finally, *Depth3* provides large sensitivities for all runoff-oriented metrics, with similar spatial patterns than those obtained with *Ws*, *Ds* and *DsMAX*, but to a smaller degree (Figure 7). *Depth3* is particularly sensitive in humid-subhumid and humid catchments, suggesting a direct relationship with mean annual precipitation. In these climatic domains, periodic heavy rainfall events enable a continuous recharge of the second and third soil layers – which may reach saturation- and thus a constant baseflow generation that affects runoff response and the retention time of soil moisture, producing higher baseflow during wet seasons (Shi et al., 2008).

4.3.2 Evaporative processes

The evaluation metrics associated with these processes are RR (a measure of the overall water balance) and TRANSP (plant transpiration), being *LAI*, *Rmin*, *Expt2* and *Depth2* the most important parameters.

Figure 7 shows a pronounced spatial variability in *LAI* sensitivities across a large domain that comprises very different land cover types. One can note that *LAI* yields high sensitivities for nearly all hydroclimatic regimes, since this parameter controls the evaporation from the canopy layer and canopy transpiration. In hyperarid climates, the *LAI* is usually less important, given the permanent water stress common for grid cells with bare soil. In summary, *LAI* is influential wherever vegetation exists, regardless of the prevailing hydroclimatic regime.

The parameter *Rmin* yields parametric sensitivities across humid-subhumid and humid areas (Figure 7 and Table 6). In the canopy resistance process, there is a stomatal resistance multiplier, $g_{sm}[n]$, defined as a soil moisture stress factor that depends on the water in the root zone for the *n*-th surface cover class. Thus, when the soil moisture in layer *n* is less than the fraction of the moisture content at the wilting point, the value of $g_{sm}[n]$ is 0, while when the soil moisture is greater than the fractional content of soil moisture at the critical point (~ 70% of field capacity), the value of $g_{sm}[n]$ is 1. For the intermediate condition, $g_{sm}[n]$ values vary linearly with soil moisture in that layer, which explains why *Rmin* provides high sensitivities in very humid (i.e., large precipitation) climates.

Finally, our results show that *Expt2* and *Depth2* yield large sensitivities to RR and TRANSP in all hydroclimatic regimes, since they affect the soil moisture content in layer 2, which indirectly affects the $g_{sm}[n]$ factor in the canopy resistance formulation. These parameters show a lower relative sensitivity in humid-subhumid and humid climates, since the *Rmin* parameter becomes more relevant when there is no soil moisture stress (i.e., $g_{sm}[n] \sim 1$).

4.3.3 Snow processes

Figure 7 shows that *NEWALB*, *ALBTHA* and *ALBAA* yield high sensitivities throughout the study domain, especially in areas where snow processes dominate hydrological responses. In particular, the *NEWALB* parameter is important throughout the domain and reaches the highest values for snow-oriented evaluation metrics. Additionally, the results in Figure 7 show that *ALBAA* and *ALBTHA* dominate snow responses in different domains: the *ALBTHA* parameter yields large sensitivities in humid and sub-humid mountain areas located southern from 34° S, with large effects on the snow season length and the maximum SWE accumulation, while *ALBAA* shows greater sensitivity for the other climatic regimes, affecting SnowLength and sublimation in semiarid, colder environments in Northern Chile (26°-29° S).

5 Conclusions

We have characterized parameter sensitivities provided by the Variable Infiltration Capacity hydrological model. To this end, we have implemented the DELSA method at every 0.05°×0.05° (~5 km) grid cell contained in 101 basins across continental Chile (i.e., a total of 5,574 grid cells), spanning a broad diversity of hydroclimatic (from hyper-arid to humid) and physiographic (e.g., topography, land cover) conditions. Our experiments consider a suite of 43 parameters included in

soil, vegetation and snow process representations, with three of these corresponding to hard-coded parameters (i.e., not exposed to model users). We use eight model evaluation metrics that account for runoff components, evapotranspiration and snow processes, and conduct correlation analyses to disentangle relationships between parametric sensitivities and pixel-scale attributes. The main findings of this study are as follows:

- The results indicate that 31 out of 43 parameters (i.e., 72%) yield little or no sensitivity, most of which correspond to soil and vegetation processes. Therefore, calibrating such parameters will lead to minimal improvements in system representations with considerable computational costs.
- The three evaluation metrics focused on snow accumulation and ablation processes were found to be highly sensitive to hard-coded parameters. Exposing these parameters will certainly expand our abilities to perform extensive analysis and increase our opportunities to improve model fidelity and characterize model uncertainty.
- For some evaluation metrics, the climate attributes examined here are highly correlated with parameter sensitivities, which therefore inherit spatial patterns observed in climate variables across the territory. In particular, mean annual precipitation and the aridity index are highly correlated with *Ds*, *Ws* and *DsMAX* sensitivities when examining RMSE, TRMSE and FMS. Unexpectedly, temperature yields a relatively small influence, even for metrics and parameters associated with snow processes. The rest of the attributes (topographic, soil and land cover) provided generally low correlations, and therefore small predictive power on parameter sensitivities.
- Parametric sensitivities are strongly related with the climate types in the case study basins. In humid environments, the most important parameters are related to the third soil layer (*Ws*; *Ds*; *DsMAX* and *Depth3*) and vegetation (*Rmin*); in arid regimes, the most influential parameters are associated with the firsts soils layers (*INFILT*; *Expt2*; and *Depth2*).
- In snow-dominated areas, the hard-coded parameters *NEWALB*; *ALBTHA* and *ALBAA* provide large sensitivities to maximum SWE, snow season length and sublimation.
- The leaf area index (*LAI*) is a crucial parameter wherever there is vegetation on the ground, especially if it presents an overstory. Although such condition is more frequent in humid environments, the relevance of this parameter depends on vegetation characteristics rather than the underlying climatic conditions.

Overall, our study contributes to the existing literature by providing guidance on relevant VIC parameters for a suite of target processes and climate types, using a large number of modeling units at a relatively high (~5 km) spatial resolution. Future studies aiming at improving spatial calibration density with VIC – or any similar hydrology or land surface model – could incorporate this information to define target parameters, and examine to what extent the spatial patterns in parameter sensitivities relate to calibrated parameter fields. Finally, the strong correlations found here between parameter sensitivities and hydroclimatic properties reaffirm the need to incorporate periods with contrasting climate characteristics in sensitivity analysis, in order to design better calibration strategies for climate impact studies.

Acknowledgments

Pablo A. Mendoza received support from Fondecyt Project 11200142 and CONICYT/PIA Project AFB180004. Powered@NLHPC: This research was partially supported by the supercomputing infrastructure of the NLHPC (ECM-02).

III. CONCLUSIONES

En este trabajo de tesis, se presentó una caracterización de las sensibilidades de los parámetros del modelo hidrológico VIC a través del método DELSA. El análisis de sensibilidad se lleva a cabo en 5.574 celdas con resolución horizontal de 0,05°×0,05° (~ 5 km), contenidas en 101 cuencas de Chile continental, abarcando una amplia diversidad de características hidroclimáticas y fisiográficas. Los experimentos numéricos consideraron un total de 43 parámetros de suelo, vegetación y nieve, donde tres de ellos corresponden a parámetros 'codificados' (es decir, no expuestos a los usuarios del modelo). Se utilizan ocho métricas de evaluación que consideran procesos relacionados con caudal, evapotranspiración y manto nival, y se efectúa un análisis de correlación para determinar las relaciones entre las sensibilidades paramétricas y los atributos a la escala de celda. Los principales hallazgos de este estudio son los siguientes:

- Los resultados indican que 31 de 43 parámetros (es decir, 72%) entregan poca o ninguna sensibilidad, la mayoría de los cuales corresponde a parámetros de suelo y vegetación. Por lo tanto, la incorporación de dichos parámetros en el proceso de calibración conducirá a mejoras mínimas en las representaciones del sistema, con considerables costos computacionales.
- Se encontró que las tres métricas de evaluación enfocadas en los procesos de nieve y ablación eran altamente sensibles a los parámetros codificados. La exposición de estos parámetros, sin duda, ampliará las capacidades para realizar análisis exhaustivos y mejorar la fidelidad del modelo, así como caracterizaciones de incertidumbre paramétrica.
- Para algunas métricas de evaluación, los atributos climáticos examinados están altamente correlacionados con las sensibilidades de los parámetros, por lo cual los patrones espaciales observados resultan comparables. En particular, la precipitación media anual y el índice de aridez están altamente correlacionados con los parámetros *Ds*, *Ws* y *DsMAX* cuando se examinan RMSE, TRMSE y FMS. Contrariamente a las expectativas, la temperatura tiene una influencia relativamente pequeña, incluso para métricas y parámetros asociados con los procesos de nieve. El resto de los atributos (topográficos, de suelo y cobertura del suelo) proporcionaron correlaciones generalmente bajas y, por lo tanto, un poder predictivo menor sobre la sensibilidad de los parámetros.
- Las sensibilidades paramétricas están fuertemente relacionadas con los tipos de clima en las cuencas del estudio analizadas. En ambientes húmedos, los parámetros más importantes están relacionados con la tercera capa de suelo (*Ws*; *Ds*; *DsMAX* y *Depth3*) y la vegetación (*Rmin*); en los regímenes áridos, los parámetros más influyentes están asociados con las primeras capas de suelo (*INFILT*; *Expt2*; y *Depth2*).
- En áreas dominadas por la nieve, los parámetros no expuestos al usuario *NEWALB*; *ALBTHA* y *ALBAA* proporcionan una gran sensibilidad al SWE máximo, la duración de la temporada de nieve y la sublimación. Estos parámetros están involucrados en el balance energético de la capa superficial de la nieve y en la tasa de decaimiento del albedo de la nieve.
- El índice de área foliar (*LAI*) es un parámetro crucial en cualquier lugar con cobertura vegetal, especialmente si esta presenta dosel arbóreo (*overstory*) o región superior de copas de árboles, tal como bosques o selvas. Si bien esta condición es más habitual en ambientes húmedos, la importancia de este parámetro responde a las características de la vegetación, que no necesariamente se correlacionan con patrones climáticos.

La principal contribución de este estudio es la identificación de sensibilidades paramétricas del modelo VIC, incluyendo un considerable número de parámetros (estándares y codificados) y una alta densidad espacial (~5 km), junto con la caracterización de patrones espaciales e interpretación de procesos a lo largo del territorio nacional. Los resultados indican que 12 (de 43) parámetros del modelo VIC son "sensibles" y que, por lo tanto, deben incluirse en la etapa de calibración del modelo. además, los resultados presentados aquí constituyen una guía sobre los parámetros relevantes de acuerdo a los procesos de interés del/la modelador(a) y el tipos de clima imperante dentro del dominio de interés.

Finalmente, las fuertes correlaciones reportadas en este estudio entre las sensibilidades de los parámetros y las propiedades hidroclimáticas reafirman la necesidad de incorporar períodos con características climáticas contrastantes en el análisis de sensibilidad, con el fin de diseñar mejores estrategias de calibración para aplicaciones de diversa índole que involucren al modelo VIC, por ejemplo, estudios de impactos de cambio climático en recursos hídricos.

BIBLIOGRAFÍA

Abbaspour, K. C., Rouholahnejad, E., Vaghefi, S., Srinivasan, R., Yang, H. and Kløve, B.: A continental-scale hydrology and water quality model for Europe: Calibration and uncertainty of a high-resolution large-scale SWAT model, J. Hydrol., 524, 733–752, doi:10.1016/j.jhydrol.2015.03.027, 2015.

Addor, N. and Melsen, L. A.: Legacy, Rather Than Adequacy, Drives the Selection of Hydrological Models, Water Resour. Res., 55(1), 378–390, doi:10.1029/2018WR022958, 2019.

Addor, N., Nearing, G., Prieto, C., Newman, A. J., Le Vine, N. and Clark, M. P.: A Ranking of Hydrological Signatures Based on Their Predictability in Space, Water Resour. Res., 54(11), 8792–8812, doi:10.1029/2018WR022606, 2018.

Alvarez-garreton, C., Mendoza, P. A., Boisier, J. P., Addor, N., Galleguillos, M., Zambrano-bigiarini, M., Lara, A., Puelma, C., Cortes, G. and Garreaud, R.: The CAMELS-CL dataset : catchment attributes and meteorology for large sample studies – Chile dataset, , 5817–5846, 2018.

Andreadis, K. M., Storck, P. and Lettenmaier, D. P.: Modeling snow accumulation and ablation processes in forested environments, Water Resour. Res., 45(5), 1–13, doi:10.1029/2008WR007042, 2009.

Arheimer, B., Pimentel, R., Isberg, K., Crochemore, L., Andersson, J. C. M., Hasan, A. and Pineda, L.: Global catchment modelling using World-Wide HYPE (WWH), open data, and stepwise parameter estimation, Hydrol. Earth Syst. Sci., 24(2), 535–559, doi:10.5194/hess-24-535-2020, 2020.

Bastidas, L. A., Gupta, H. V, Sorooshian, S., Shuttleworth, W. J. and Yang, Z. L.: Sensitivity analysis of a land surface scheme using multicriteria methods, J. Geophys. Res., 104, 19,481-19,490, 1999.

Bastidas, L. A., Hogue, T. S., Sorooshian, S., Gupta, H. V. and Shuttleworth, W. J.: Parameter sensitivity analysis for different complexity land surface models using multicriteria methods, J. Geophys. Res., 111, D20101, doi:10.1029/2005JD006377, 2006.

Beck, H. E., van Dijk, A. I. J. M., de Roo, A., Miralles, D. G., McVicar, T. R., Schellekens, J. and

Bruijnzeel, L. A.: Global-scale regionalization of hydrologic model parameters, Water Resour. Res., 52(5), 3599–3622, doi:10.1002/2015WR018247, 2016.

Bennett, K. E., Urrego Blanco, J. R., Jonko, A., Bohn, T. J., Atchley, A. L., Urban, N. M. and Middleton, R. S.: Global Sensitivity of Simulated Water Balance Indicators Under Future Climate Change in the Colorado Basin, Water Resour. Res., 54(1), 132–149, doi:10.1002/2017WR020471, 2018.

Berg, P., Donnelly, C. and Gustafsson, D.: Near-real-time adjusted reanalysis forcing data for hydrology, Hydrol. Earth Syst. Sci., 22(2), 989–1000, doi:10.5194/hess-22-989-2018, 2018.

Beven, K.: Changing ideas in hydrology — The case of physically-based models, J. Hydrol., 105(1–2), 157–172, doi:10.1016/0022-1694(89)90101-7, 1989.

Blondin, C.: Parameterization of Land-Surface Processes in Numerical Weather Prediction, L. Surf. Evaporation, 31–54, doi:10.1007/978-1-4612-3032-8_3, 1991.

Bohn, T. J. and Vivoni, E. R.: Process-based characterization of evapotranspiration sources over the North American monsoon region, Water Resour. Res., 52(1), 358–384, doi:10.1002/2015WR017934, 2016.

Boisier, J. P., Alvarez-Garretón, C., Cepeda, J., Osses, A., Vásquez, N. and Rondanelli, R.: CR2MET: A high-resolution precipitation and temperature dataset for hydroclimatic research in Chile, EGUGA, 20, 19739 [online] Available from: https://ui.adsabs.harvard.edu/abs/2018EGUGA..2019739B/abstract (Accessed 8 July 2021), 2018.

Boyle, D. P., Gupta, H. V., Sorooshian, S., Koren, V., Zhang, Z. and Smith, M.: Toward improved streamflow forecasts: Value of semidistributed modeling, Water Resour. Res., 37(11), 2749–2759, doi:10.1029/2000WR000207, 2001.

Brooks, R. and Corey, A.: Hydraulic properties of porous media, Hydrol. Pap. Color. State Univ., 3(March), 37 pp [online] Available from: http://www.citeulike.org/group/1336/article/711012, 1964.

Budyko, M. I.: Climate and Life., 1974.

Carpenter, T. M. and Georgakakos, K. P.: Intercomparison of lumped versus distributed hydrologic model ensemble simulations on operational forecast scales, J. Hydrol., 329(1–2), 174–185, doi:10.1016/j.jhydrol.2006.02.013, 2006.

Casper, M. C., Grigoryan, G., Gronz, O., Gutjahr, O., Heinemann, G., Ley, R. and Rock, A.: Analysis of projected hydrological behavior of catchments based on signature indices, Hydrol. Earth Syst. Sci., 16(2), 409–421, doi:10.5194/hess-16-409-2012, 2012.

Chaney, N. W., Herman, J. D., Reed, P. M. and Wood, E. F.: Flood and drought hydrologic monitoring: The role of model parameter uncertainty, Hydrol. Earth Syst. Sci., 19(7), 3239–3251, doi:10.5194/hess-19-3239-2015, 2015.

Chawla, I. and Mujumdar, P. P.: Isolating the impacts of land use and climate change on streamflow, Hydrol. Earth Syst. Sci., 19(8), 3633–3651, doi:10.5194/hess-19-3633-2015, 2015.

Chegwidden, O. S. S., Nijssen, B., Rupp, D. E. E., Arnold, J. R. R., Clark, M. P. P., Hamman, J.

J. J., Kao, S. C. S. C., Mao, Y., Mizukami, N., Mote, P. W., Pan, M., Pytlak, E. and Xiao, M.: How do modeling decisions affect the spread among hydrologic climate change projections? Exploring a large ensemble of simulations across a diversity of hydroclimates, Earth's Futur., 7(6), 623–637, doi:10.1029/2018EF001047, 2019.

Chen, F., Barlage, M., Tewari, M., Rasmussen, R., Jin, J., Lettenmaier, D., Livneh, B., Lin, C., Miguez-Macho, G., Niu, G., Wen, L. and Yang, Z.: Modeling seasonal snowpack evolution in the complex terrain and forested Colorado Headwaters region: A model intercomparison study, J. Geophys. Res. Atmos., 119(24), 13,795-13,819, doi:10.1002/2014JD022167, 2014.

Cherkauer, K. A., Bowling, L. C. and Lettenmaier, D. P.: Variable infiltration capacity cold land process model updates, Glob. Planet. Change, 38(1–2), 151–159, doi:10.1016/S0921-8181(03)00025-0, 2003.

Chipman, H. A., George, E. I. and McCulloch, R. E.: BART: Bayesian additive regression trees, Ann. Appl. Stat., 4(1), 266–298, doi:10.1214/09-AOAS285, 2010.

Clark, M. P., Nijssen, B., Lundquist, J. D., Kavetski, D., Rupp, D. E., Woods, R. A., Freer, J. E., Gutmann, E. D., Wood, A. W., Brekke, L. D., Arnold, J. R., Gochis, D. J. and Rasmussen, R. M.: A unified approach for process-based hydrologic modeling: 1. Modeling concept, Water Resour. Res., doi:10.1002/2015WR017198, 2015.

Clark, M. P., Bierkens, M. F. P., Samaniego, L., Woods, R. A., Uijlenhoet, R., Bennett, K. E., Pauwels, V. R. N., Cai, X., Wood, A. W. and Peters-Lidard, C. D.: The evolution of process-based hydrologic models: historical challenges and the collective quest for physical realism, Hydrol. Earth Syst. Sci., 21(7), 3427–3440, doi:10.5194/hess-21-3427-2017, 2017.

Copernicus Climate Change Service: ERA5: Fifth generation of ECMWF atmospheric reanalyses of the global climate, 2017.

Cosby, B. J., Hornberger, G. M., Clapp, R. B. and Ginn, T. R.: A Statistical Exploration of the Relationships of Soil Moisture Characteristics to the Physical Properties of Soils, Water Resour. Res., 20(6), 682–690, doi:10.1029/WR020i006p00682, 1984.

Cuntz, M., Mai, J., Samaniego, L., Clark, M., Wulfmeyer, V., Branch, O., Attinger, S. and Thober, S.: The impact of standard and hard-coded parameters on the hydrologic fluxes in the Noah-MP land surface model, J. Geophys. Res. Atmos., 121(18), 10,676-10,700, doi:10.1002/2016JD025097, 2016.

DeChant, C. M. and Moradkhani, H.: Toward a reliable prediction of seasonal forecast uncertainty: Addressing model and initial condition uncertainty with ensemble data assimilation and Sequential Bayesian Combination, J. Hydrol., 519, 2967–2977, doi:10.1016/j.jhydrol.2014.05.045, 2014.

Dee, D. P., Uppala, S. M., Simmons, A. J., Berrisford, P., Poli, P., Kobayashi, S., Andrae, U., Balmaseda, M. A., Balsamo, G., Bauer, P., Bechtold, P., Beljaars, A. C. M., van de Berg, L., Bidlot, J., Bormann, N., Delsol, C., Dragani, R., Fuentes, M., Geer, A. J., Haimberger, L., Healy, S. B., Hersbach, H., Hólm, E. V., Isaksen, L., Kållberg, P., Köhler, M., Matricardi, M., Mcnally, A. P., Monge-Sanz, B. M., Morcrette, J. J., Park, B. K., Peubey, C., de Rosnay, P., Tavolato, C., Thépaut, J. N. and Vitart, F.: The ERA-Interim reanalysis: Configuration and performance of the data assimilation system, Q. J. R. Meteorol. Soc., 137(656), 553–597, doi:10.1002/qj.828, 2011.

Demaria, E. M., Nijssen, B. and Wagener, T.: Monte Carlo sensitivity analysis of land surface parameters using the Variable Infiltration Capacity model, J. Geophys. Res. Atmos., 112(11), 1–15, doi:10.1029/2006JD007534, 2007.

DGA: Actualización del Balance Hídrico Nacional, SIT N° 417, Santiago, Chile., 2017.

DGA: Aplicación de la Metodología de Actualización del Balance Hídrico Nacional en las Cuencas de las Macrozonas Norte y Centro, SIT N° 435, Santiago, Chile., 2018.

DGA: Aplicación de La Metodología de Actualización del Balance Hídrico Nacional en las Cuencas de la Macrozona Sur y Parte de la Macrozona Austral, SIT N° 441, Santiago, Chile., 2019.

DGA: Aplicación de la Metodología de Actualización del Balance Hídrico Nacional en las Cuencas de la Parte Sur de la Macrozona Austral e Isla de Pascua, SIT N° 444, Santiago, Chile., 2020.

Do, H. X., Gudmundsson, L., Leonard, M. and Westra, S.: The Global Streamflow Indices and Metadata Archive (GSIM)-Part 1: The production of a daily streamflow archive and metadata, Earth Syst. Sci. Data, 10(2), 765–785, doi:10.5194/essd-10-765-2018, 2018.

Dorman, J. and Sellers, P.: A global climatology of albedo, roughness length and stomatal resistance for atmospheric general circulation models as represented by the simple biosphere model (SiB), J. Appl. Meteorol., 28, 833–855, 1989.

Ducoudré, N. I., Laval, K. and Perrier, A.: SECHIBA, a New Set of Parameterizations of the Hydrologic Exchanges at the Land-Atmosphere Interface within the LMD Atmospheric General Circulation Model, J. Clim., 6(2), 248–273, doi:10.1175/1520-0442(1993)006<0248:sansop>2.0.co;2, 1993.

Foglia, L., Hill, M. C., Mehl, S. W. and Burlando, P.: Sensitivity analysis, calibration, and testing of a distributed hydrological model using error-based weighting and one objective function, Water Resour. Res., 45(6), W06427, doi:10.1029/2008WR007255, 2009.

Franchini, M. and Pacciani, M.: Comparative analysis of several conceptual rainfall-runoff models, J. Hydrol., 122(1–4), 161–219, doi:10.1016/0022-1694(91)90178-K, 1991.

Friedman, J. H.: Multivariate Adaptive Regression Splines, Ann. Stat., 19(1), 590–606, doi:10.1214/aos/1176347963, 1991.

Gates, D. M. and Evans, L. T.: Environmental Control of Plant Growth., Bull. Torrey Bot. Club, 91(3), 235, doi:10.2307/2483533, 1964.

Ghiggi, G., Humphrey, V., Seneviratne, S. and Gudmundsson, L.: GRUN: An observations-based global gridded runoff dataset from 1902 to 2014, GRUN An Obs. Glob. gridded runoff dataset from 1902 to 2014, 1–32, doi:10.5194/essd-2019-32, 2019.

Göhler, M., Mai, J. and Cuntz, M.: Use of eigendecomposition in a parameter sensitivity analysis of the Community Land Model, J. Geophys. Res. Biogeosciences, 118(2), 904–921, doi:10.1002/jgrg.20072, 2013.

Gou, J., Miao, C., Duan, Q., Tang, Q., Di, Z., Liao, W., Wu, J. and Zhou, R.: Sensitivity Analysis-

Based Automatic Parameter Calibration of the VIC Model for Streamflow Simulations Over China, Water Resour. Res., 56(1), 1–19, doi:10.1029/2019WR025968, 2020.

van Griensven, A., Meixner, T., Grunwald, S., Bishop, T., Diluzio, M. and Srinivasan, R.: A global sensitivity analysis tool for the parameters of multi-variable catchment models, J. Hydrol., 324(1–4), 10–23, doi:10.1016/j.jhydrol.2005.09.008, 2006.

Hamman, J. J., Nijssen, B., Bohn, T. J., Gergel, D. R. and Mao, Y.: The variable infiltration capacity model version 5 (VIC-5): Infrastructure improvements for new applications and reproducibility, Geosci. Model Dev., 11(8), 3481–3496, doi:10.5194/gmd-11-3481-2018, 2018.

Hengl, T., De Jesus, J. M., Heuvelink, G. B. M., Gonzalez, M. R., Kilibarda, M., Blagotić, A., Shangguan, W., Wright, M. N., Geng, X., Bauer-Marschallinger, B., Guevara, M. A., Vargas, R., MacMillan, R. A., Batjes, N. H., Leenaars, J. G. B., Ribeiro, E., Wheeler, I., Mantel, S. and Kempen, B.: SoilGrids250m: Global gridded soil information based on machine learning., 2017.

Hogue, T. S., Bastidas, L., Gupta, H., Sorooshian, S., Mitchell, K. and Emmerich, W.: Evaluation and transferability of the Noah land surface model in semiarid environments, J. Hydrometeorol., 6(1), 68–84, 2005.

Hornberger, G. M. and Spear, R. C.: Approach to the preliminary analysis of environmental systems, J. Environ. Mgmt, 12:1, 7–18 [online] Available from: https://www.osti.gov/biblio/6396608, 1981.

Hou, Z., Huang, M., Leung, L. R., Lin, G. and Ricciuto, D. M.: Sensitivity of surface flux simulations to hydrologic parameters based on an uncertainty quantification framework applied to the Community Land Model, J. Geophys. Res. Atmos., 117(15), 1–18, doi:10.1029/2012JD017521, 2012.

Hrachowitz, M., Savenije, H. H. G., Blöschl, G., McDonnell, J. J., Sivapalan, M., Pomeroy, J. W., Arheimer, B., Blume, T., Clark, M. P., Ehret, U., Fenicia, F., Freer, J. E., Gelfan, A., Gupta, H. V., Hughes, D. A., Hut, R. W., Montanari, A., Pande, S., Tetzlaff, D., Troch, P. A., Uhlenbrook, S., Wagener, T., Winsemius, H. C., Woods, R. A., Zehe, E. and Cudennec, C.: A decade of Predictions in Ungauged Basins (PUB)-a review, Hydrol. Sci. J., 58(6), 1198–1255, doi:10.1080/02626667.2013.803183, 2013.

Huang, M. and Liang, X.: On the assessment of the impact of reducing parameters and identification of parameter uncertainties for a hydrologic model with applications to ungauged basins, J. Hydrol., 320(1–2), 37–61, doi:10.1016/j.jhydrol.2005.07.010, 2006.

Lawrence, D. M., Fisher, R. A., Koven, C. D., Oleson, K. W., Swenson, S. C., Bonan, G., Collier, N., Ghimire, B., van Kampenhout, L., Kennedy, D., Kluzek, E., Lawrence, P. J., Li, F., Li, H., Lombardozzi, D., Riley, W. J., Sacks, W. J., Shi, M., Vertenstein, M., Wieder, W. R., Xu, C., Ali, A. A., Badger, A. M., Bisht, G., van den Broeke, M., Brunke, M. A., Burns, S. P., Buzan, J., Clark, M., Craig, A., Dahlin, K., Drewniak, B., Fisher, J. B., Flanner, M., Fox, A. M., Gentine, P., Hoffman, F., Keppel-Aleks, G., Knox, R., Kumar, S., Lenaerts, J., Leung, L. R., Lipscomb, W. H., Lu, Y., Pandey, A., Pelletier, J. D., Perket, J., Randerson, J. T., Ricciuto, D. M., Sanderson, B. M., Slater, A., Subin, Z. M., Tang, J., Thomas, R. Q., Val Martin, M. and Zeng, X.: The Community Land Model Version 5: Description of New Features, Benchmarking, and Impact of Forcing Uncertainty, J. Adv. Model. Earth Syst., 11(12), 4245–4287, doi:10.1029/2018MS001583, 2019.

Liang, X. and Guo, J.: Intercomparison of land-surface parameterization schemes: Sensitivity of surface energy and water fluxes to model parameters, J. Hydrol., 279(1–4), 182–209, doi:10.1016/S0022-1694(03)00168-9, 2003.

Liang, X., Lettenmaier, D. P., Wood, E. F. and Burges, S. J.: A simple hydrologically based model of land surface water and energy fluxes for general circulation models, J. Geophys. Res., 99(D7), 14415, doi:10.1029/94JD00483, 1994.

Liang, X., Wood, E. F. and Lettenmaier, D. P.: Surface soil moisture parameterization of the VIC-2L model: Evaluation and modification, Glob. Planet. Change, 13(1–4), 195–206, doi:10.1016/0921-8181(95)00046-1, 1996.

Lilhare, R., Pokorny, S., Déry, S. J., Stadnyk, T. A. and Koenig, K. A.: Sensitivity analysis and uncertainty assessment in water budgets simulated by the variable infiltration capacity model for Canadian subarctic watersheds, Hydrol. Process., 34(9), 2057–2075, doi:10.1002/hyp.13711, 2020.

Liu, Y. and Gupta, H. V.: Uncertainty in hydrologic modeling: Toward an integrated data assimilation framework, Water Resour. Res., 43(7), 1–18, doi:10.1029/2006WR005756, 2007.

Marks, D. and Dozier, J.: Climate and energy exchange at the snow surface in the Alpine Region of the Sierra Nevada: 2. Snow cover energy balance, Water Resour. Res., 28(11), 3043–3054, doi:10.1029/92WR01483, 1992.

Massoud, E. C., Xu, C., Fisher, R. A., Knox, R. G., Walker, A. P., Serbin, S. P., Christoffersen, B. O., Holm, J. A., Kueppers, L. M., Ricciuto, D. M., Wei, L., Johnson, D. J., Chambers, J. Q., Koven, C. D., McDowell, N. G. and Vrugt, J. A.: Identification of key parameters controlling demographically structured vegetation dynamics in a land surface model: CLM4.5(FATES), Geosci. Model Dev., 12(9), 4133–4164, doi:10.5194/gmd-12-4133-2019, 2019.

McCabe, M. F., Rodell, M., Alsdorf, D. E., Miralles, D. G., Uijlenhoet, R., Wagner, W., Lucieer, A., Houborg, R., Verhoest, N. E. C., Franz, T. E., Shi, J., Gao, H. and Wood, E. F.: The future of Earth observation in hydrology, Hydrol. Earth Syst. Sci., 21(7), 3879–3914, doi:10.5194/hess-21-3879-2017, 2017.

Melsen, L., Teuling, A., Torfs, P., Zappa, M., Mizukami, N., Clark, M. and Uijlenhoet, R.: Representation of spatial and temporal variability in large-domain hydrological models: Case study for a mesoscale pre-Alpine basin, Hydrol. Earth Syst. Sci., 20(6), 2207–2226, doi:10.5194/hess-20-2207-2016, 2016.

Melsen, L. A., Teuling, A. J., Torfs, P. J. J. F., Zappa, M., Mizukami, N., Mendoza, P. A., Clark, M. P. and Uijlenhoet, R.: Subjective modeling decisions can significantly impact the simulation of flood and drought events, J. Hydrol., 568(November 2018), 1093–1104, doi:10.1016/j.jhydrol.2018.11.046, 2019.

Mendoza, P. A., Clark, M. P., Barlage, M., Rajagopalan, B., Samaniego, L., Abramowitz, G. and Gupta, H.: Are we unnecessarily constraining the agility of complex process-based models?, Water Resour. Res., 51(1), 716–728, doi:10.1002/2014WR015820, 2015a.

Mendoza, P. A., Clark, M. P., Mizukami, N., Newman, A. J., Barlage, M., Gutmann, E. D., Rasmussen, R. M., Rajagopalan, B., Brekke, L. D. and Arnold, J. R.: Effects of hydrologic model

choice and calibration on the portrayal of climate change impacts, J. Hydrometeorol., 16(2), 762–780, doi:10.1175/JHM-D-14-0104.1, 2015b.

Misirli, F., Gupta, H. V, Sorooshian, S. and Thiemann, M.: Bayesian recursive estimation of parameter and output uncertainty for watershed models, vol. 6, edited by Q. Duan, H. V. Gupta, S. Sorooshian, A. N. Rousseau, and R. Turcotte, pp. 113–124, American Geophysical Union, Washington, D. C., 2003.

Mitchell, K. E., Lohmann, D., Houser, P. R., Wood, E. F., Schaake, J. C., Robock, A., Cosgrove, B. A., Sheffield, J., Duan, Q., Luo, L., Higgins, W., Pinker, R. T., Tarpley, J. D., Lettenmaier, D. P., Marshall, C. H., Entin, J. K., Pan, M., Shi, W., Koren, V., Meng, J., Ramsay, B. H. and Bailey, A. A.: The multi-institution North American Land Data Assimilation System (NLDAS): Utilizing multiple GCIP products and partners in a continental distributed hydrological modeling system, J. Geophys. Res., 109(D7), D07S90, doi:10.1029/2003JD003823, 2004.

Mizukami, N., P. Clark, M., G. Slater, A., D. Brekke, L., M. Elsner, M., R. Arnold, J. and Gangopadhyay, S.: Hydrologic Implications of Different Large-Scale Meteorological Model Forcing Datasets in Mountainous Regions, J. Hydrometeorol., 15(1), 474–488, doi:10.1175/JHM-D-13-036.1, 2014.

Mizukami, N., Clark, M. P., Gutmann, E. D., Mendoza, P. A., Newman, A. J., Nijssen, B., Livneh, B., Hay, L. E., Arnold, J. R. and Brekke, L. D.: Implications of the Methodological Choices for Hydrologic Portrayals of Climate Change over the Contiguous United States: Statistically Downscaled Forcing Data and Hydrologic Models, J. Hydrometeorol., 17(1), 73–98, doi:10.1175/JHM-D-14-0187.1, 2016.

Montgomery, D. C.: Design and analysis of experiments, Wiley., 1991.

Morris, M. D.: Factorial sampling plans for preliminary computational experiments, Technometrics, 33(2), 161–174, doi:10.1080/00401706.1991.10484804, 1991.

Muleta, M. K. and Nicklow, J. W.: Sensitivity and uncertainty analysis coupled with automatic calibration for a distributed watershed model, J. Hydrol., 306(1–4), 127–145, doi:10.1016/j.jhydrol.2004.09.005, 2005.

Myneni, R. B., Ramakrishna, R., Nemani, R. and Running, S. W.: Estimation of global leaf area index and absorbed par using radiative transfer models, IEEE Trans. Geosci. Remote Sens., 35(6), 1380–1393, doi:10.1109/36.649788, 1997.

Al Nakshabandi, G. and Kohnke, H.: Thermal conductivity and diffusivity of soils as related to moisture tension and other physical properties, Agric. Meteorol., 2(4), 271–279, doi:10.1016/0002-1571(65)90013-0, 1965.

Nash, J. and Sutcliffe, J.: River flow forecasting through conceptual models part I - A discussion of principles, J. Hydrol., 10(3), 282–290, doi:10.1016/0022-1694(70)90255-6, 1970.

Nijssen, B. and Bastidas, L. A.: Land-Atmosphere Models for Water and Energy Cycle Studies, Encycl. Hydrol. Sci., 1–13, doi:10.1002/0470848944.hsa212, 2005.

Niu, G.-Y., Yang, Z.-L., Mitchell, K. E., Chen, F., Ek, M. B., Barlage, M., Kumar, A., Manning, K., Niyogi, D., Rosero, E., Tewari, M. and Xia, Y.: The community Noah land surface model with multiparameterization options (Noah-MP): 1. Model description and evaluation with local-scale

measurements, J. Geophys. Res., 116(D12), D12109, doi:10.1029/2010JD015139, 2011.

Oubeidillah, A. A., Kao, S. C., Ashfaq, M., Naz, B. S. and Tootle, G.: A large-scale, high-resolution hydrological model parameter data set for climate change impact assessment for the conterminous US, Hydrol. Earth Syst. Sci., 18(1), 67–84, doi:10.5194/hess-18-67-2014, 2014.

Pi, H. and Peterson, C.: Finding the Embedding Dimension and Variable Dependencies in Time Series, Neural Comput., 6(3), 509–520, doi:10.1162/neco.1994.6.3.509, 1994.

Pokhrel, P. and Gupta, H. V.: On the use of spatial regularization strategies to improve calibration of distributed watershed models, Water Resour. Res., 46(1), W01505, doi:10.1029/2009WR008066, 2010.

Prihodko, L., Denning, A. S. S., Hanan, N. P. P., Baker, I. and Davis, K.: Sensitivity, uncertainty and time dependence of parameters in a complex land surface model, Agric. For. Meteorol., 148(2), 268–287, doi:10.1016/j.agrformet.2007.08.006, 2008.

Rakovec, O., Hill, M. C., Clark, M. P., Weerts, A. H., Teuling, A. J. and Uijlenhoet, R.: Distributed evaluation of local sensitivity analysis (DELSA), with application to hydrologic models, Water Resour. Res., 50(1), 409–426, doi:10.1002/2013WR014063, 2014.

Rawls, W. J., Ahuja, L. R. and Brakensiek, D. L. Shirmohammadi, A.: Infiltration and soil water movement, in Handbook of hydrology, edited by D. R. Maidment, p. pp.5.1-5.51, McGraw-Hill Inc., New York. [online] Available from: https://www.cabdirect.org/cabdirect/abstract/19931982563, 1992.

Razavi, S. and Gupta, H. V.: What do we mean by sensitivity analysis? the need for comprehensive characterization of "global" sensitivity in Earth and Environmental systems models, Water Resour. Res., 51(5), 3070–3092, doi:10.1002/2014WR016527, 2015.

Razavi, S. and Gupta, H. V.: A new framework for comprehensive, robust, and efficient global sensitivity analysis: 2. Application, Water Resour. Res., 52(1), 423–439, doi:10.1002/2015WR017558, 2016.

Reba, M. L., Marks, D., Link, T. E., Pomeroy, J. and Winstral, A.: Sensitivity of model parameterizations for simulated latent heat flux at the snow surface for complex mountain sites, Hydrol. Process., 28(3), 868–881, doi:10.1002/hyp.9619, 2014.

Reynolds, C. A., Jackson, T. J. and Rawls, W. J.: Estimating soil water-holding capacities by linking the Food and Agriculture Organization soil map of the world with global pedon databases and continuous pedotransfer functions, Water Resour. Res., 36(12), 3653–3662, doi:10.1029/2000WR900130, 2000.

Rosero, E., Yang, Z. L., Gulden, L. E., Niu, G. Y. and Gochis, D. J.: Evaluating enhanced hydrological representations in Noah LSM over transition zones: Implications for model development, J. Hydrometeorol., 10(3), 600–622, doi:10.1175/2009JHM1029.1, 2009.

Rosero, E., Yang, Z.-L., Wagener, T., Gulden, L. E., Yatheendradas, S. and Niu, G.-Y.: Quantifying parameter sensitivity, interaction, and transferability in hydrologically enhanced versions of the Noah land surface model over transition zones during the warm season, J. Geophys. Res., 115(D3), 1–21, doi:10.1029/2009JD012035, 2010.

Rosolem, R., Gupta, H. V., Shuttleworth, W. J., Zeng, X. and de Gonçalves, L. G. G.: A fully multiple-criteria implementation of the Sobol′ method for parameter sensitivity analysis, J. Geophys. Res., 117(D7), 1–18, doi:10.1029/2011JD016355, 2012.

Saltelli, A., Ratto, M., Andres, T., Campolongo, F., Cariboni, J., Gatelli, D., Saisana, M. and Tarantola, S.: Global Sensitivity Analysis. The Primer., 2008.

Schmied, H. M., Eisner, S., Franz, D., Wattenbach, M., Portmann, F. T., Flörke, M. and Döll, P.: Sensitivity of simulated global-scale freshwater fluxes and storages to input data, hydrological model structure, human water use and calibration, Hydrol. Earth Syst. Sci., 18(9), 3511–3538, doi:10.5194/hess-18-3511-2014, 2014.

Shi, X., Wood, A. W. and Lettenmaier, D. P.: How essentialis hydrologic model calibration to seasonal stream flow forecasting?, J. Hydrometeorol., 9(6), 1350–1363, doi:10.1175/2008JHM1001.1, 2008.

Sobol', I. M.: Global sensitivity indices for nonlinear mathematical models and their Monte Carlo estimates, Math. Comput. Simul., 55, 271–280, 2001.

Sobol', I. M. and Kucherenko, S.: A new derivative based importance criterion for groups of variables and its link with the global sensitivity indices, Comput. Phys. Commun., 181(7), 1212–1217, doi:10.1016/j.cpc.2010.03.006, 2010.

Sorooshian, S. and Chu, W.: Review of parameterization and parameter estimation for hydrologic models, L. Surf. Obs. Model. Data Assim., (2001), 127–140, doi:10.1142/9789814472616_0005, 2013.

Tian, S., Tregoning, P., Renzullo, L. J., van Dijk, A. I. J. M., Walker, J. P., Pauwels, V. R. N. and Allgeyer, S.: Improved water balance component estimates through joint assimilation of GRACE water storage and SMOS soil moisture retrievals, Water Resour. Res., 53(3), 1820–1840, doi:10.1002/2016WR019641, 2017.

Todini, E.: The ARNO rainfall-runoff model, J. Hydrol., 175(1–4), 339–382, doi:10.1016/S0022-1694(96)80016-3, 1996.

Todini, E.: Hydrological catchment modelling: Past, present and future, Hydrol. Earth Syst. Sci., 11(1), 468–482, doi:10.5194/hess-11-468-2007, 2007.

Tonkin, M. J. and Doherty, J.: A hybrid regularized inversion methodology for highly parameterized environmental models, Water Resour. Res., 41(10), 1–16, doi:10.1029/2005WR003995, 2005.

Troy, T. J., Wood, E. F. and Sheffield, J.: An efficient calibration method for continental-scale land surface modeling, Water Resour. Res., 44(9), 1–13, doi:10.1029/2007WR006513, 2008.

UNEP: World atlas of desertification.. ed. 2, edited by N. Middleton and D. Thomas, Arnold, Hodder Headline, PLC. [online] Available from: https://agris.fao.org/agris-search/search.do?recordID=GB1997034137, 1997.

USACE: Snow hydrology: Summary report of the snow investigations, North Pacific Division, Corps of Engineers, U.S. Army. [online] Available from: https://usace.contentdm.oclc.org/digital/collection/p266001coll1/id/4172/, 1956.

Vano, J. A. and Lettenmaier, D. P.: A sensitivity-based approach to evaluating future changes in Colorado River discharge, Clim. Change, 122(4), 621–634, doi:10.1007/s10584-013-1023-x, 2014.

VanShaar, J. R., Haddeland, I. and Lettenmaier, D. P.: Effects of land-cover changes on the hydrological response of interior Columbia River basin forested catchments, Hydrol. Process., 16(13), 2499–2520, doi:10.1002/hyp.1017, 2002.

Vásquez, N., Cepeda, J., Gómez, T., Mendoza, P. A., Lagos, M., Boisier, J. P., Álvarez-Garretón, C. and Vargas, X.: Catchment-Scale Natural Water Balance in Chile, in Water Resources of Chile, pp. 189–208., 2021.

Verbist, K., Santibañez, F., Gabriels, D. and Soto, G.: Documento Técnico Nº 25. Atlas de Zonas Áridas de América Latina y el Caribe., 2010.

Vořechovský, M.: Hierarchical Refinement of Latin Hypercube Samples, Comput. Civ. Infrastruct. Eng., 30(5), 394–411, doi:10.1111/mice.12088, 2015.

Wang, Z., Zhong, R., Lai, C., Zeng, Z., Lian, Y. and Bai, X.: Climate change enhances the severity and variability of drought in the Pearl River Basin in South China in the 21st century, Agric. For. Meteorol., 249(September 2017), 149–162, doi:10.1016/j.agrformet.2017.12.077, 2018.

Wi, S., Ray, P., Demaria, E. M. C., Steinschneider, S. and Brown, C.: A user-friendly software package for VIC hydrologic model development, Environ. Model. Softw., 98, 35–53, doi:10.1016/j.envsoft.2017.09.006, 2017.

Wood, A. W., Kumar, A. and Lettenmaier, D. P.: A retrospective assessment of National Centers for Environmental prediction climate model-based ensemble hydrologic forecasting in the western United States, J. Geophys. Res. D Atmos., 110(4), 1–16, doi:10.1029/2004JD004508, 2005.

Wood, E. F., Lettenmaier, D. P. and Zartarian, V. G.: A land-surface hydrology parameterization with subgrid variability for general circulation models, J. Geophys. Res., 97(D3), 2717–2728, doi:10.1029/91JD01786, 1992.

Wood, E. F., Roundy, J. K., Troy, T. J., van Beek, L. P. H., Bierkens, M. F. P., Blyth, E., de Roo, A., Döll, P., Ek, M., Famiglietti, J., Gochis, D., van de Giesen, N., Houser, P., Jaffé, P. R., Kollet, S., Lehner, B., Lettenmaier, D. P., Peters-Lidard, C., Sivapalan, M., Sheffield, J., Wade, A. and Whitehead, P.: Hyperresolution global land surface modeling: Meeting a grand challenge for monitoring Earth's terrestrial water, Water Resour. Res., 47(5), 2515–2542, doi:10.1029/2010WR010090, 2011.

Woodward, J. L.: Estimating the Flammable Mass of a Vapor Cloud, John Wiley & Sons, Inc., Hoboken, NJ, USA., 1999.

Xia, Y., Mitchell, K., Ek, M., Sheffield, J., Cosgrove, B., Wood, E., Luo, L., Alonge, C., Wei, H., Meng, J., Livneh, B., Lettenmaier, D., Koren, V., Duan, Q., Mo, K., Fan, Y. and Mocko, D.: Continental-scale water and energy flux analysis and validation for the North American Land Data Assimilation System project phase 2 (NLDAS-2): 1. Intercomparison and application of model products, J. Geophys. Res., 117(D3), D03109, doi:10.1029/2011JD016048, 2012.

Xie, Z., Yuan, F., Duan, Q., Zheng, J., Liang, M. and Chen, F.: Regional parameter estimation of the VIC land surface model: Methodology and application to river basins in China, J.

Hydrometeorol., 8(3), 447–468, doi:10.1175/JHM568.1, 2007.

Yadav, M., Wagener, T. and Gupta, H.: Regionalization of constraints on expected watershed response behavior for improved predictions in ungauged basins, Adv. Water Resour., 30(8), 1756–1774, doi:10.1016/j.advwatres.2007.01.005, 2007.

Yang, Y., Pan, M., Beck, H. E., Fisher, C. K., Beighley, R. E., Kao, S. C., Hong, Y. and Wood, E. F.: In Quest of Calibration Density and Consistency in Hydrologic Modeling: Distributed Parameter Calibration against Streamflow Characteristics, Water Resour. Res., 55(9), 7784–7803, doi:10.1029/2018WR024178, 2019.

Yang, Z.-L., Niu, G.-Y., Mitchell, K. E., Chen, F., Ek, M. B., Barlage, M., Longuevergne, L., Manning, K., Niyogi, D., Tewari, M. and Xia, Y.: The community Noah land surface model with multiparameterization options (Noah-MP): 2. Evaluation over global river basins, J. Geophys. Res., 116(D12), 1–16, doi:10.1029/2010JD015140, 2011.

Yeste, P., García-Valdecasas Ojeda, M., Gámiz-Fortis, S. R., Castro-Díez, Y. and Esteban-Parra, M. J.: Integrated sensitivity analysis of a macroscale hydrologic model in the north of the Iberian Peninsula, J. Hydrol., 590(September 2019), 125230, doi:10.1016/j.jhydrol.2020.125230, 2020.

Zegers, G., Mendoza, P. A., Garces, A. and Montserrat, S.: Sensitivity and identifiability of rheological parameters in debris flow modeling, Nat. Hazards Earth Syst. Sci., 20(7), 1919–1930, doi:10.5194/nhess-20-1919-2020, 2020.

Zhang, D., Chen, X., Yao, H. and Lin, B.: Improved calibration scheme of SWAT by separating wet and dry seasons, Ecol. Modell., 301, 54–61, doi:10.1016/j.ecolmodel.2015.01.018, 2015.

Zhao, R.-J., Zuang, Y.-L., Fang, L.-R., Liu, X.-R. and Zhang, Q.-S.: Xinanjiang Model., IAHS-AISH Publ., (129), 351–356, 1980.

Zink, M., Kumar, R., Cuntz, M. and Samaniego, L.: A high-resolution dataset of water fluxes and states for Germany accounting for parametric uncertainty, Hydrol. Earth Syst. Sci., 21(3), 1769–1790, doi:10.5194/hess-21-1769-2017, 2017.